

11-18  
391556

# TECHNICAL NOTE

D-923

AN AUTOMATIC TERMINAL GUIDANCE SYSTEM FOR RENDEZVOUS

WITH A SATELLITE

By Terrance M. Carney

Langley Research Center  
Langley Field, Va.

NATIONAL AERONAUTICS AND SPACE ADMINISTRATION  
WASHINGTON

August 1961



## NATIONAL AERONAUTICS AND SPACE ADMINISTRATION

## TECHNICAL NOTE D-923

## AN AUTOMATIC TERMINAL GUIDANCE SYSTEM FOR RENDEZVOUS

## WITH A SATELLITE

By Terrance M. Carney

## SUMMARY

L  
1  
5  
2  
2

This study includes a consideration of the design philosophy for an automatic terminal guidance system, a derivation of guidance equations required, and an outline of the general type of instrumentation necessary to provide the essential information. A control system for a sample vehicle is analyzed.

A representative case, rendezvous with a satellite in circular orbit at 400 nautical miles, was examined. Terminal-stage nominal burning times of 200 and 400 seconds were used.

For the 200-second case, initial errors in circumferential displacement of  $\pm 25,000$  feet, in radial displacement of 7,000 to -9,000 feet, and in lateral displacement of  $\pm 20,000$  feet were within the capabilities of the system. Velocity errors of 300 to -400 ft/sec in the circumferential direction, 180 to -200 ft/sec in the radial direction, and velocity offsets of at least  $2^\circ$  ( $\pm 800$  ft/sec) in the lateral direction could also be handled. The 400-second case was capable of correcting larger errors, but limits were not determined.

The dependence of required characteristic velocity on initial errors was determined and it was found that increases over the nominal terminal-stage characteristic velocity of the order of 15 percent covered most of the previously mentioned in-plane errors. The requirements were more severe for cases with lateral velocity offsets. A simplified set of guidance equations was tested and produced only slight variations in performance.

Overall velocity requirements and mass ratios were determined for terminal-stage burning times of 100, 200, 300, and 400 seconds and for a range of transfer angles by using exact calculations for the terminal stage and an impulsive launching velocity. These results indicated that the shortest burning time consistent with the launch guidance errors expected gave the best mass ratio.

## INTRODUCTION

One of the many problems engendered by space operations is that of physical communication between orbiting space stations and the earth. The most straightforward means of accomplishing this communication is by direct launch of a vehicle from earth and subsequent guidance into coincidence in velocity and position with the orbiting station. This problem and the corollary problems of bringing orbiting vehicles together in space (orbital transfer) and of matching position but not the velocity of the station (hard rendezvous) have received much attention in the recent literature. References 1 to 6 are representative of work being done in this area.

The overall problem of launch and guidance of a vehicle to rendezvous is one of large scale and is best handled by tearing it into several phases. A reasonable partitioning is into launch, midcourse guidance, terminal guidance, and docking. There is a strong interaction between these phases which must always be checked, but for first considerations this separation is convenient.

This paper will be concerned with the terminal guidance stage, which is here defined to commence with onboard sensor acquisition of the target vehicle prior to firing of the final stage and to extend to the beginning of the docking phase. Both automatic and piloted systems have previously been proposed for this task (refs. 1, 3, and 4); only the automatic approach will be treated here.

Included in this study is a consideration of the design philosophy for a terminal guidance system, a derivation of guidance equations required, and suggestions for the general type of instrumentation required to provide the necessary information.

The following steps were taken in the design and examination of this system:

1. Closed-form solutions were written for simplified equations of motion.

2. These solutions were compared with exact numerical solutions to determine that no gross errors had been introduced by the simplifications.

3. Guidance relations were formed from the analytical solutions by substitution of measured variables.

4. A control technique for steering the rendezvous vehicle toward the trajectory defined by the guidance relations was devised and analyzed.

L  
1  
5  
2  
2

5. A typical case was examined by programing simplified equations of motion for the IBM type 704 electronic data processing machine and testing the proposed system for a variety of initial errors with respect to a nominal initial aim point for terminal-stage burning times of 200 and 400 seconds.

6. The penalty associated with using extended terminal-stage burning times was determined by calculating the overall mass ratio for various terminal-stage burning times plus an associated impulsive launch.

## SYMBOLS

The axis system and conventions used in this report are illustrated in figures 1, 2, and 3. The symbols used are defined as follows:

$A$	constant in guidance equations
$c$	effective rocket exhaust velocity, ft/sec
$d_x$	displacement of attitude control thruster from center of gravity along x body axis, ft
$\bar{e}$	unit vector
$f_c$	thrust per unit mass of commuter vehicle, lb/slug
$f_{ls}$	thrust per unit mass along line-of-sight projection in XY-plane, lb/slug
$f_n$	thrust per unit mass normal to line of sight in XY-plane, lb/slug
$g$	acceleration due to gravity, ft/sec <sup>2</sup>
$G$	apparent gravitational acceleration, ft/sec <sup>2</sup>
$\bar{i}$	unit vector along line-of-sight projection in XY-plane
$I_x, I_y, I_z$	moments of inertia about x, y, z body axes, respectively, slug-ft <sup>2</sup>
$I_{sp}$	specific impulse, sec
$\bar{j}$	unit vector normal to line-of-sight projection in XY-plane

$\bar{k}$	unit vector parallel to Z-axis	
$K_Z, K_Z^i$	gain constants in longitudinal controller	
$K_\beta^i$	navigation constant in lateral controller, sec	
$K_\delta$	attitude control thrust slope, lb/radian	
$\bar{l}_v$	unit vector along $\bar{V}_{c,s}$	
$m$	mass, slugs	L
$M_y, M_z$	control moments about y and z body axes, respectively, ft-lb	1
$p, q, r$	angular rates about x, y, and z body axes, respectively, radians/sec	5
$[PF]$	performance function	2
$R$	radial distance from center of earth, ft	2
$S$	control sensitivity	
$t$	time, sec	
$t_g$	time remaining to rendezvous from reference time, sec	
$\Delta t$	burning time, sec	
$T$	thrust, lb	
$u, v, w$	velocities along x, y, z body axes, respectively, ft/sec	
$V$	total velocity, ft/sec	
$\Delta V$	characteristic velocity, ft/sec	
$x, y, z$	body axes with origin at commuter center of gravity and displacements along these axes	
$X, Y, Z$	rectangular axes with origin at space station at $t = 0$ and displacements along these axes	
$\alpha$	elevation angle, radians	

$\beta$	angle of lateral offset in XY-plane, radians
$\gamma$	gravitational constant, $\text{ft}^3/\text{sec}^2$
$\delta$	attitude control valve displacement, radians
$\Delta$	error
$\epsilon$	error signal
$\zeta$	ratio of damping to critical damping
$\eta_x, \eta_y, \eta_z$	total impulse consumed by axial, yaw control, and pitch control thrusters, lb-sec
$\theta, \psi, \phi$	Euler angles, radians
$\lambda$	Laplace operator
$\mu$	mass ratio, ratio of mass at launch to final mass
$\rho$	line-of-sight range, ft
$\sigma$	lateral velocity offset angle, deg
$\tau$	characteristic time, sec
$\tilde{\psi}$	yaw angle with respect to line of sight, radians
$\omega$	natural frequency, radians/sec
$\Omega$	angle of transfer, deg
$\Omega_T$	angle of transfer from launch to initiation of terminal stage, deg

## Subscripts:

c	commuter
cl	closed loop
com	command
cs	control system
e	earth

f	at rendezvous	
i	at initiation of terminal stage	
I	inertial reference	
ls	line of sight	
L	yaw servo gain	
meas	measured	L
n	normal	1
nom	nominal initial condition	5
o	at reference $t = 0$	2
ol	open loop	2
p	pitch servo gain	
q	pitch rate gain	
r	yaw rate gain	
R	radial	
s	space station	
t	circumferential	
x,y,z	along or about x-, y-, or z-axes, respectively	
X,Y,Z	along or about X-, Y-, or Z-axes, respectively	
$\theta$	pitch angle gain	
$\psi$	yaw angle gain	

A dot over a variable indicates a derivative with respect to time; two dots indicate a second derivative with respect to time.

A bar over a variable indicates a vector.



## ANALYSIS

### System Philosophy

The ideal terminal guidance system is one that follows a nominal path which is optimum from the fuel-consumption standpoint, allows correction of gross errors in initial conditions without instability or excessive additional fuel use, and employs highly reliable instrumentation in minimum quantity. It is clear that these criteria must be compromised to produce a system which will best satisfy them in combination. This can be illustrated by the contrast between the optimum-fuel-consumption path, which consists of an impulsive boost to orbital velocity at apogee of the launch trajectory, and the best path for error correction, which consists of a very long low-acceleration burning period during which the thrust vector can be controlled. The impulsive boost admits of no displacement-error correction capability, while the low-acceleration path is rather inefficient from the standpoint of fuel consumption. Again, a complete inertial reference offers the possibility of very sophisticated steering techniques, but introduces drift error problems as well as weight and volume penalties, while simple proportional navigation requires no fixed reference but steers a path which is not the most economical of fuel.

The terminal guidance system of this paper was developed around a variable-thrust rocket motor, since control of both direction and magnitude of the thrust vector provides maximum flexibility in correction of errors. The philosophy adopted in the design of the system was that a path requiring the least steering of the commuter vehicle should be used, that the thrust demanded during flight should be a smooth, slowly varying function, and that the simplest reference possible should be employed.

### Mass Particle Solution

In order to meet the requirements of minimum steering and a smooth thrust function, the nominal flight path was defined as one where constant thrust was maintained in a constant direction with respect to a local earth reference. The simplest case, rendezvous with a station in circular orbit, was chosen because it is most amenable to closed-form solutions.

A solution to simplified equations of motion of a particle with constant thrust and linear mass variation with time was undertaken to study this flight path. These equations were written in a rectangular axis system (fig. 1) where it was assumed that the motion of the target

or space station is linear along the X-axis. It was further assumed that the force of gravity is constant in the neighborhood of the space station, and centrifugal effects were introduced by modifying the gravity term. The equations are:

$$\ddot{X} = \frac{T_X}{m_O + \dot{m}t} \quad (1)$$

$$\ddot{Y} = \frac{T_Y}{m_O + \dot{m}t} \quad (2)$$

$$\ddot{Z} = \frac{T_Z}{m_O + \dot{m}t} + \frac{1}{R_s} (V_s^2 - \dot{X}^2) \quad (3)$$

In reference 7 it is shown that thrusting along the velocity vector of the vehicle is an efficient method of gaining velocity. In the terminal stage of rendezvous with stations in nearly circular orbit the velocity vector lies substantially in the local horizontal plane. Since the local horizontal is a convenient reference and some complication is involved in determining the true velocity direction, thrusting in the horizontal plane provides a good approximation to the efficient course and is relatively simple to mechanize. Therefore  $T_Y$  and  $T_Z$  were set equal to zero and the relationship between  $T_X$  and  $\dot{m}$  written

$$T_X = -\dot{m}c \quad (4)$$

where  $c$  is the effective rocket exhaust velocity. A solution in the XZ-plane is obtained first. The required end conditions are

$$\dot{X}(t_f) = V_s$$

$$X(t_f) - V_s t_f = 0$$

$$Z(t_f) = \dot{Z}(t_f) = 0$$

where  $t_f$  is defined as the time at rendezvous. Equations (1) and (3) were integrated and these required end conditions applied to obtain the following closed-form solutions for the required geometrical initial conditions in terms of burning rate  $\dot{m}$  and remaining flight time  $t_g$ .

$$\dot{X}_O = V_s + c \log_e \left( 1 + \frac{\dot{m}}{m_O} t_g \right) \quad (5)$$

$$X_O = c \left[ \frac{m_O}{\dot{m}} \log_e \left( 1 + \frac{\dot{m}}{m_O} t_g \right) - t_g \right] \quad (6)$$

$$\begin{aligned} \dot{Z}_O = & \frac{1}{R_S} \left[ \dot{X}_O^2 - v_s^2 + 2c(\dot{X}_O + c) \right] t_g \\ & - \frac{2c}{R_S \dot{m}} \left[ \dot{X}_O + c - \frac{c}{2} \log_e \left( 1 + \frac{\dot{m}}{m_O} t_g \right) \right] (m_O + \dot{m} t_g) \log_e \left( 1 + \frac{\dot{m}}{m_O} t_g \right) \end{aligned} \quad (7)$$

$$\begin{aligned} Z_O = & - \left[ \dot{Z}_O - \frac{c}{R_S} \frac{m_O}{\dot{m}} \left( \dot{X}_O + \frac{3c}{2} \right) \right] t_g - \frac{1}{2R_S} \left[ v_s^2 - \dot{X}_O^2 - 3c \left( \dot{X}_O + \frac{7c}{6} \right) \right] t_g^2 \\ & - \frac{c}{R_S \dot{m}^2} \left( \dot{X}_O + \frac{3c}{2} \right) (m_O + \dot{m} t_g)^2 \log_e \left( 1 + \frac{\dot{m}}{m_O} t_g \right) \\ & + \frac{c^2}{2R_S \dot{m}^2} (m_O + \dot{m} t_g)^2 \left[ \log_e \left( 1 + \frac{\dot{m}}{m_O} t_g \right) \right]^2 \end{aligned} \quad (8)$$

Inspection of these four equations reveals that fixing any two of the six parameters  $\dot{X}_O$ ,  $X_O$ ,  $\dot{Z}_O$ ,  $Z_O$ ,  $t_g$ , and  $\dot{m}$  defines a unique solution. The time of flight can then be selected and the initial circumferential velocity  $\dot{X}_O$  can be determined from launching trajectory considerations to calculate nominal initial conditions. In the real case, the four geometrical variables will be fixed at the time of radar acquisition. The procedure proposed is that  $\dot{X}_O$  and  $X_O$  be considered the prime variables and that measurements of these be used to compute continuously the  $Z_O$ ,  $\dot{Z}_O$ , and thrust magnitude  $T_X$  required. Appropriate directional control of the thrust vector will then be exercised to drive the measured  $Z$  and  $\dot{Z}$  to the required values. When this condition is satisfied, the commuter vehicle will be on a flight path requiring no further steering and using constant thrust in the local horizontal plane to rendezvous with the target station. The relations required, then, are  $\dot{Z}_O$ ,  $Z_O$ , and  $T_X$  in terms of  $\dot{X}_O$  and  $X_O$ . Solving equations (4) and (5) for  $T_X/\dot{m}$  gives

$$\frac{T_X}{\dot{m}_O} = \frac{c}{t_g} \left[ 1 - e^{-\left( \frac{v_s - \dot{X}_O}{c} \right)} \right] \quad (9)$$

Express  $t_g$  by using equations (5) and (6) and substituting a series representation for the exponential, and manipulate equations (7), (8), and (9) to yield the following expressions:

$$\frac{T_X}{m_0} = \frac{(v_s - \dot{x}_0)^2}{2X_0} \left[ 1 - \frac{v_s - \dot{x}_0}{3c} + \frac{(v_s - \dot{x}_0)^2}{12c^2} \right] \quad (10)$$

$$\dot{z}_0 = \frac{2}{3R_s} (v_s - \dot{x}_0) X_0 \left( 1 + \frac{v_s - \dot{x}_0}{12c} \right) - \frac{2v_s}{R_s} X_0 \quad (11)$$

$$z_0 = \frac{4v_s}{3R_s} \frac{X_0^2}{v_s - \dot{x}_0} \left[ 1 - \left( 1 + \frac{3c}{v_s} \right) \frac{v_s - \dot{x}_0}{12c} + \left( 1 + \frac{c}{2v_s} \right) \frac{(v_s - \dot{x}_0)^2}{24c^2} \right] \quad (12)$$

Terms above order  $\left[ (v_s - \dot{x}_0)/c \right]^2$  have been dropped since this corresponds to order  $10^{-2}$  for the rendezvous situations considered in this paper.

In order to evaluate the assumptions used to obtain the preceding solutions, exact solutions for coplanar rendezvous with a station in a 400-nautical-mile, circular orbit with 200- and 400-second terminal-stage burning times were calculated numerically. The exact solutions were for constant thrust in the horizontal plane with the constraint that the initial circumferential velocity should match the analytical solution. The equations and techniques used in arriving at these solutions are outlined in appendix A. The geometric errors introduced by the assumptions are illustrated in figure 4. For the 200-second case the maximum radial velocity  $\dot{z}$  difference is 8 ft/sec and the maximum radial displacement  $z$  difference is 70 feet. Notice that the correspondence improves near rendezvous. The agreement for the 400-second case is not as good, showing a maximum radial velocity difference of 58 ft/sec and maximum radial displacement of 1,000 feet. In operation the system continually computes the analytic solution, and as the time to rendezvous decreases the analytic solution will approach the corresponding exact solution until near rendezvous they will be effectively coincident.

The errors in thrust required were also studied. Satisfaction of the velocity constraint mentioned previously required thrusts respectively 2.9 and 12.1 percent higher for the exact 200- and 400-second-burning-time cases than for the corresponding analytic solutions. This

thrust error is attributed to the neglect of coupling of the radial motion in the equation describing circumferential velocity gain in the simplified system. The closed-loop guidance would tend to nullify these errors since it would predict successively more accurate thrusts as the vehicles closed.

The effect of this thrust discrepancy on computed fuel consumption was also determined. Figure 5 is a plot of the ratio of characteristic velocity for the exact case to the initial circumferential velocity of the commuter relative to the station against the initial circumferential velocity difference for terminal-stage burning times of 100, 200, 300, and 400 seconds. The expression used for calculating characteristic velocity is:

$$\begin{aligned}\Delta V &= g_0 I_{sp} \log_e \left( \frac{m_0}{m_f} \right) \\ &= c \log_e \left( \frac{m_0}{m_f} \right)\end{aligned}\tag{13}$$

Inspection of equation (5) shows that the characteristic velocity calculated in the rectangularized solution will be the initial circumferential velocity relative to the station. The regularity of the variation of the ratio plotted in figure 5 indicates that simple corrections can be applied to fuel consumptions calculated in the rectangularized system to make them significant.

The next consideration was guidance in the XY-plane. The fact that the Y-dynamics were not coupled to the XZ-system led to the conclusion that offsets in  $Y$  and  $\dot{Y}$  could be handled independently of the in-plane guidance, particularly in the case where a relatively long burning time is used and rapid response is not demanded of the vehicle. Since maneuvers in the XY-plane are not coupled to gravity (to first order) the path which is followed does not strongly affect the efficiency of the system as long as the path is smooth and does not require large or frequent accelerations transverse to the X-axis. Wrigley, in reference 5, has described an application of the proportional navigation technique to satellite rendezvous. The advantage of such a system is that it does not require a measurement of bearing angle which depends on an inertial reference. Only information about the range and rate of change of range to the target and the rate of change of bearing of the line of sight is needed. This technique, when restricted to the XY-plane, was believed to be satisfactory for control of  $Y$ - and  $\dot{Y}$ -offsets. Development of this system for the current application is carried out in appendixes B and C. The control equation yielded is:

$$\tilde{\psi}_{\text{com}} = K_{\beta} \frac{\dot{\beta} \dot{\rho}}{\frac{T_x}{m}} \quad (14)$$

where  $\tilde{\psi}$  is the yaw tilt angle of the thrust vector from the line of sight in the horizontal plane.

It is clear that the elliptic case is more difficult to study analytically than is rendezvous with a station in circular orbit. It is submitted, however, that for small eccentricities this problem can be handled by biasing the XY reference plane to a direction parallel to the inclination of the desired velocity vector at rendezvous to the local horizontal. This inclination can be determined as a function of the known orbital elements of the station and the flight time plus the predicted remaining flight time  $t_g$  of the commuter vehicle.

L  
1  
5  
2  
2

### Instrumentation

In order to obtain the accuracy required in the terminal stage of rendezvous it is best to measure the guidance information in relative coordinates from onboard the commuter or station. Measurement of the required quantities from the earth would introduce a command delay time, as well as inaccuracies from long ranges and extra coordinate transformations.

The particle solutions defined the quantities which must be measured for guidance purposes. A general plan for providing these measurements was evolved and is illustrated in figure 2. The local vertical reference is provided by a horizon scanner. Radar or a similar technique is used to measure range and range rate. The elevation of the line of sight from the local horizontal must be measured. The rates of slewing of the line of sight with respect to inertial space in the XY-plane and with respect to the local horizontal in elevation are required. In the cases studied, rates of the order of a milliradian/second were encountered. To provide sufficient precision to control these rates, measurement accuracies of the order of 0.1 milliradian/second or better are required. If conventional means of rate measurement, such as mounting gyros on a radar antenna or differentiating successive angular measurements, will not yield this accuracy, an auxiliary system, such as an optical tracker, may be necessary.

Difficulties arising from the noise properties and pulsed character of the radar information and other instrument errors are not considered in this paper. It is believed that these effects can be counteracted without changing the character of the system, and that most of the measurement errors will be in part compensated by the closed-loop configuration.

The particular mission plan will determine which vehicle carries the sensing equipment. An instrumented commutator would be required for rendezvous with passive stations, while rendezvous of several commutators with one space station might make location of the sensors at the station more economical. In either case, the guidance technique described can be used.

### Guidance Equations

Once the parameters to be controlled have been expressed and the measured variables have been defined, it is necessary to develop relations for these parameters in terms of the actual sensor inputs. It is also desirable to find relations which are relatively simple to compute with onboard equipment. In order to do this, measured (line of sight) variables are introduced into the mass particle solutions for  $T_X$ ,  $Z$ ,  $\dot{Z}$ , and the lateral command quantity  $\tilde{\psi}$ . The trigonometric functions involved have been replaced by their small-angle approximations. This procedure is carried out in appendix C. The resulting expressions are:

$$Z_{\text{com}} = -\rho^2 \left[ A_1 (1 - \alpha^2) + \frac{A_2}{\dot{\rho}} \right] \quad (15)$$

$$\dot{Z}_{\text{com}} = -\rho \left[ A_3 \left( 1 - \frac{\alpha^2}{2} \right) + A_4 \dot{\rho} \right] \quad (16)$$

where

$$A_1 = \frac{V_S}{9cR_S} \left( 1 + \frac{3c}{V_S} \right)$$

$$A_2 = \frac{4V_S}{3R_S}$$

$$A_3 = \frac{2V_S}{R_S}$$

$$A_4 = \frac{2}{3R_S}$$

$$\left( \frac{T_X}{m} \right)_{\text{com}} = \frac{\dot{\rho}^2}{2\rho} \left( 1 + \frac{\dot{\rho}}{3c} - \frac{2\rho\alpha\dot{\alpha}}{\dot{\rho}} \right) \quad (17)$$

$$\tilde{v}_{com} = K_{\beta} \frac{\dot{\beta} \dot{\rho}}{\frac{T_X}{m}} \quad (18)$$

where equation (18) is equation (14) repeated.

Note that the expression for axial acceleration is similar to that used by Spradlin in reference 1.

Although these relations could be generated by a suitable analog computer, the large range covered by the variables would seem to make digital computation more appropriate. The sampled data form of the radar output also lends itself to this computation technique, since a digital computer could be used for data smoothing.

### Commuter Stability Analysis

Determination of the guidance commands led to the next requirement, a steering system to compare the commands to measured values and to correct the observed errors. The control system proposed operates by changing the commuter vehicle's attitude to provide components of the axial thrust in the proper direction to correct error signals generated by the guidance computer. The magnitude of the main engine thrust is determined by equation (17) without compensation for pitch or yaw angles. Attitude control is provided by a set of four thrusters at the nose of the vehicle. (See fig. 3.) Roll stabilization of the vehicle with respect to the local horizontal is assumed. This mode of control was chosen to avoid the complication of gimbaling the main rocket, and because it was slightly less complex than a pure torque attitude controller, which requires four additional thrusters.

An elementary analysis of the dynamics of the controlled vehicle was carried out by means of the root-locus technique to determine means of stabilizing the vehicle and system gains which provide satisfactory response. Block diagrams of the longitudinal and lateral controllers investigated appear in figure 6 and the analysis appears in appendix D. It was necessary to compromise between requiring such low system gains that no initial errors could upset the vehicle and providing high enough gains to insure rapid tracking near the end of the terminal stage. Normally, this is best achieved by use of variable gains or nonlinear compensation. The generalized system considered in this paper used linear gains with limits on the error signals. These limits were arbitrarily set so that no tilt in pitch greater than 0.6 radian or tilt in yaw greater than 0.5 radian could be called for. The maximum force-to-mass ratio of the attitude-control thrusters was also limited to 0.25 pound per slug to maintain a reasonable sizing relative to the main motor.



These limits were checked only to determine their effect on stability, and no attempt was made to attain the optional limited system.

## RESULTS AND DISCUSSION

In order to demonstrate the flexibility of this terminal guidance concept and to detect any inherent problems in its usage, a particular rendezvous case was tested. The case chosen was terminal rendezvous with a station in 400-nautical-mile circular orbit. Nominal initial conditions were based on an  $82.5^\circ$  transfer from impulsive launch. Reference 6 points out that a transfer of this order offers advantages in frequency of possible rendezvous, and the orbital altitude was selected as representative for a space station. A commuter vehicle with a mass of 300 slugs was assumed with reasonable associated physical characteristics.

The equations of motion in body axes were programed for numerical solution on the IBM type 704 electronic data processing machine, and solutions were carried out in terms of the rectangular reference axes previously discussed. The equations and physical characteristics of the system studied are included in appendix E. This scheme was employed rather than exact equations to simplify the programing and because the previously noted investigation had shown the geometric errors introduced to be reasonable and had indicated that a simple linear correction (see fig. 5) applied to the fuel consumption measured in the simplified system would make it correspond well to exact values. Moreover, most of the data computed were evaluated on a comparative basis so that deviations of the nominal values from the exact cases did not affect any conclusions.

Nominal terminal-stage burning times of 200 and 400 seconds were studied, with emphasis on the 200-second case. Although introduction of errors changes the burning time, all cases related to a given nominal burning time will be referred to by the nominal time for convenience. For the 200-second case, the acceptable XZ-plane error perturbations in velocity and displacement from the nominal initial conditions were determined. Two lateral velocity offsets, corresponding to the conditions where the commuter velocity was  $1^\circ$  and  $2^\circ$  out of the orbital plane of the station, and various side displacements were also studied. The relation of initial side displacement to initial lateral velocity offset for minimum fuel consumption was determined. Comparable coplanar and offset cases were run for the 400-second burning time. Nominal initial conditions for these cases appear in table I. The fuel consumption was expressed as a characteristic terminal velocity requirement for all these cases to determine variations with initial errors. A simplified version of the guidance scheme was tested for the 200-second

case to determine efficiency loss due to leaving out some of the terms. Finally, the overall mass ratio variation with terminal burning time was determined by including an impulsive launch.

### In-Plane Capability

The initial error correction capability of the system was checked by the simple technique of perturbing each initial condition with successively larger errors until the system was no longer able to correct itself. This is not representative of the real case, where errors will generally occur in combination, but does indicate limits without the difficulty of determining the most probable error combinations.

Figures 7 and 8 illustrate trajectories and thrust profiles for nominal initial conditions and limiting errors for the 200-second burning time. Figure 7 shows the nominal trajectory and four error perturbations in initial displacement, while figure 8 shows the nominal trajectory and four error perturbations in initial velocity. Velocities and displacements shown are measured relative to the space station. For this case, the range of acceptable circumferential errors is 25,000 to -25,000 feet in displacement and 300 to -400 ft/sec in velocity. The radial-error range is somewhat more restrictive, being 7,000 to -9,000 feet in displacement and 180 to -200 ft/sec in velocity. The 400-second case was checked for the same extremes as the 200-second case. This case is theoretically capable of correcting larger velocity and displacement errors during its longer operating time, but its limits were not determined.

Inspection of the thrust time histories for the various errors in figures 7(a) and 8(a) reveals that the ratio of maximum to minimum thrust required is 3.25. This is well within the 5:1 range of modulation reported in reference 8 for an operating variable-thrust rocket motor. The smooth character of the thrust profiles indicates that the dynamic response demanded of the throttling system is relatively slow.

Figures 7(b) and 8(b) are time histories of the last 10 seconds before rendezvous. These are included to show the magnitude of the closing velocities and displacements in more detail, and to indicate the size of residual errors to be expected. No residual velocities greater than 1 ft/sec or displacements greater than 5 feet were encountered. However, the large closing velocities shortly before rendezvous indicate that a bias should be introduced to avoid collision of the vehicles due to measurement errors. If this bias were used, the computer would rendezvous with a point a short distance ahead of the station, and the docking system could then perform vernier corrections and direct coupling of the vehicles.

The limiting factor in these cases proved to be control-system stability. For large inputs, the limited system behaved as an on-off controller and, with the control sensitivities used, the system tended to switch too frequently and did not succeed in nullifying the  $Z$  and  $\dot{Z}$  errors before the space station closed on the commuter for initial errors outside the stated bounds. In reference 9, Schmidt outlines a technique for designing a nonlinear compensator which operates on the error signal to force the limited system to follow the optimum switching solution. For a particular system, application of this procedure should considerably improve the response of the controller and extend its error-handling capability.

Attitude-control-system impulse requirements were calculated for all cases and never exceed 1,000 pound-seconds for the proportional system used. Variations at this level are insignificant compared to variations in fuel consumption of the main motor.

### Cross-Plane Capability

The ability of the system to handle velocity offsets of  $1^\circ$  and  $2^\circ$  was tested for a range of initial displacements. Figure 9 shows the  $1^\circ$  offset case for a nominal burning time of 200 seconds. Values of  $K_\beta$ , the navigation constant, from 2.0 to 7.0 were tested. Marginal stability was exhibited for  $K_\beta = 2.0$ . Curves are plotted for  $K_\beta = 3.0$  and 7.0 to illustrate variations due to gain change. Comparison of fuel consumption for stable values indicated that  $K_\beta = 3.0$  was most economical, and no significant difference between values could be seen from a stability standpoint. For any cases tested with cross-plane errors, the initial conditions were adjusted so that the longitudinal guidance system detected no initial errors. There was little apparent coupling of the motion in the two planes during any of the cases for errors within the system limitations.

It was determined from inspection of fuel-consumption variation that the optimum initial condition for the offset case was that the initial angular rate of the line of sight be zero, that is,

$$\dot{\beta}_0 = \frac{\dot{Y}_0 X_0 + Y_0 (\dot{V}_s - \dot{X}_0)}{X_0^2 + Y_0^2} = 0 \quad (19)$$

or

$$Y_0 = \frac{X_0}{\dot{X}_0 - \dot{V}_s} \dot{Y}_0 \quad (20)$$

Inspection of the thrust time histories in figure 9 shows that the optimum initial condition ( $Y_1 = 39,537$ ) demands nearly constant thrust throughout. Comparison with the nominal case for coplanar rendezvous in figures 7 and 8 shows that a nearly constant increment of additional thrust amounting to about 10 percent is required to correct the velocity offset.

If the optimum initial condition is defined as nominal, the system is capable of handling initial Y-displacements of  $\pm 20,000$  feet for initial velocity offsets of  $0^\circ$ ,  $1^\circ$  ( $\dot{Y}_0 = -408.2$  ft/sec), or  $2^\circ$  ( $\dot{Y}_0 = -816.5$  ft/sec). Time histories of the final 10 seconds before rendezvous appear in figure 10. These are for the  $2^\circ$  lateral velocity offset case, which yields larger residual errors than the  $1^\circ$  offset case. Final velocities as large as 9 ft/sec and displacements up to 8 feet occurred for the most severe errors. This result further indicates that a bias should be introduced to prevent collision of the vehicles. The error correction capability in the cross-plane case is determined by the maximum available lateral thrust of the system at the prescribed-limit yaw tilt of 0.5 radian. Methods of increasing this tolerance were not sought, since it was already rather broad. Larger velocity offsets were not tested, and again the 400-second-burning-time case should yield larger initial tolerances but was not tested.

L  
1  
5  
2  
2

#### Characteristic Velocity Variation With Initial Errors

In order to illustrate the dependence of fuel consumption on initial errors, the characteristic velocities required for the conditions tested are plotted in figures 11(a) and 11(b). The characteristic velocities were calculated by using equation (13) and were based on the mass ratios from the computer runs. No corrections were introduced. This form is intended to generalize the results as much as possible since it removes direct dependence on specific impulse. Although the particular effective exhaust velocity used ( $c = 10,000$ ) will affect the results due to coupling of the rate of change of mass in the gravity field, mass ratios based on the included data and scaled to specific impulses in this neighborhood should be good approximations.

The variation of required characteristic velocity with errors plotted in figure 11(a) shows that the in-plane errors generate almost linear slopes, with the exception of the variation with initial vertical velocity which is roughly parabolic. If it can be guaranteed that the circumferential velocity will be low by no more than 150 ft/sec, the maximum errors require 15 percent additional characteristic velocity for the 200-second-burning-time case. For the 400-second case, the same errors require 13.2 percent additional characteristic velocity, and since this case is based on a lower nominal value, there is an additional savings in magnitude of the added velocity required.

For the cases with lateral velocity offsets the sharp increase in required characteristic velocity which occurs with increasing offset angle is illustrated in figure 11(b). The variation of required velocity with displacement errors is also large, particularly for the 200-second-burning-time case. The 400-second case is more tolerant of displacement errors in the lateral plane and performs comparably for the velocity offsets. The comparative percentages of additional characteristic velocity required to correct a  $2^\circ$  velocity offset are 18.3 percent for the 200-second case, and 21.3 percent for the 400-second case, although the additional magnitude remains about the same. For the worst lateral displacement situation,  $\pm 20,000$  feet about the nominal for the  $2^\circ$  velocity offset, the percentages of characteristic velocity which must be added are 6.5 percent for the 200-second case and 3.6 percent for the 400-second case.

### Simplified Guidance Equations

A simplified guidance technique was also tested to determine the importance of the corrective terms retained in the normal guidance relations. The only changes involved the equations for computing  $T_x/m$ , the  $Z$  and  $\dot{Z}$  commands, and for generating the measured  $Z$  and  $\dot{Z}$  from the radar data. Equations (15), (16), and (17) were simplified to

$$\frac{T_x}{m_0} = \frac{\dot{\rho}^2}{2\rho}$$

$$Z_{\text{com}} = -\rho^2 \left( A_1 + \frac{A_2}{\dot{\rho}} \right)$$

$$\dot{Z}_{\text{com}} = -\rho (A_3 + A_4 \dot{\rho})$$

and  $Z_{\text{meas}}$  and  $\dot{Z}_{\text{meas}}$  from appendix E were simplified to

$$Z_{\text{meas}} = \rho \alpha$$

$$\dot{Z}_{\text{meas}} = \dot{\rho} \alpha + \rho \dot{\alpha}$$

Only the nominal case and the extreme errors were tested by use of this system. Table II is a comparison of performance for the normal and simplified cases. For most of the coplanar cases, a small increase in fuel consumption was required by the simplified system for large errors. For the offset-velocity cases, the simplified system appeared to be slightly more economical for large errors.

Comparative evaluation of these two systems leads to the conclusion that in most cases the simplified system would be indicated. For large vehicles and particular error probabilities, the increased instrumentation weight of the normal system might be indicated.

### Overall Mass-Ratio Determination

The variation of overall mass ratio (fuel consumption) with burning time of the terminal stage can be determined only by looking at the entire energy requirement for launch and rendezvous. In order to simplify this evaluation, an impulsive launch was considered. The constraint applied to the comparison was that the transfer angle from launch to the initiation of terminal-stage burning should be the same for each burning time.

Figure 12(a) is a plot of the variation in characteristic-velocity requirements at launch and at rendezvous as a function of the angle of transfer from launch to the commencement of terminal guidance for the coplanar case with terminal-stage burning times ranging from 100 to 400 seconds and for the two-impulse case. Empirical relations were developed from the previously described exact calculations and used with Keplerian orbital relationships to compute the required characteristic velocities. Details of this work appear in appendix A.

These characteristic-velocity requirements are not significant without estimates of the efficiency of the launch and terminal stages. Accordingly, a comparison of the overall mass ratios was made subject to the assumption that the launch velocity is gained at a specific impulse of 270 seconds and the terminal velocity is gained at a specific impulse of 311 seconds. The relation used to calculate mass ratio was

$$\mu = e^{\left( \frac{V_o}{gI_{sp,1}} + \frac{\Delta V}{gI_{sp,2}} \right)}$$

The variation of mass ratio with transfer angle is shown in figure 12(b). As expected, the two-impulse transfer is the most efficient. However, this is an idealized case and practical considerations will require a burning time of some length, particularly for the high terminal-stage velocity gains dictated by the optimum mass-ratio transfer angles indicated in the figure for the impulsive case and the shorter burning times. The percentage increase from the optimum two-impulse transfer to the optimum 400-second terminal-stage-burning transfer is the order of 1 percent. In the real case the best burning time would be the minimum capable of correcting the errors expected in launch guidance. When

L  
1  
5  
2  
2

compared with the shortest burning time practical, the penalty associated with adding time to correct errors will generally be much less than 1 percent.

L  
1  
5  
2  
2

The variation of mass ratio with lateral offset was determined at the  $82.5^\circ$  transfer angle studied for the impulsive, the 200-second-burning-time, and the 400-second-burning-time cases. The 200- and 400-second cases were run in the rectangular axes discussed previously since they were controlled. The characteristic velocities derived from the computations for these two cases were amplified by the ratio of characteristic velocity required for the exact nominal case to that required for the nominal case in rectangular axes to make their magnitudes significantly comparable to the impulsive case. The linearity of the plot of the ratio of characteristic velocity required against initial-circumferential-velocity difference in figure 5 indicates that this is a valid weighting technique.

The mass ratios resulting from this calculation are plotted in figure 13. The impulsive case is again the most efficient, and it is seen that the mass-ratio penalty for longer burning times increases with the velocity offset angles.

#### CONCLUDING REMARKS

The intent of this paper is to describe an automatic terminal guidance concept for satellite rendezvous and to illustrate some of the steps necessary to implement the system. The guidance system described has a nominal mode of operation, using constant thrust in the local horizontal plane to close the velocity difference in the terminal stage of direct-ascent rendezvous with an orbiting space station. Initial condition errors for the terminal stage will generally occur as a result of launch guidance inaccuracies. The system nullifies these errors by varying the magnitude and direction of the thrust according to commands calculated from onboard measurements of the relative position and velocity of the vehicles. A control scheme for tracking these commands was devised and its dynamics analyzed.

Sample calculations were made for a particular case, rendezvous with a satellite in 400-nautical-mile circular orbit for an  $82.5^\circ$  transfer angle. The range of initial errors with respect to a nominal aim point which the system could correct was determined. The limiting factor was system stability. For a 200-second terminal-stage burning time, initial circumferential errors of  $\pm 25,000$  feet in displacement and 300 to -400 ft/sec in velocity, and radial errors of 7,000 to -9,000 feet in displacement and 180 to -200 ft/sec in velocity could be corrected. Lateral velocities were tested only for offset angles

up to  $2^\circ$ , and it was found that displacements of  $\pm 20,000$  feet from the nominal aim point could be corrected for all cases. The 400-second case demonstrated capability to correct larger errors. Provision of about 200 ft/sec additional terminal-stage characteristic-velocity capability (15 percent additional) was sufficient to handle all the in-plane errors if the initial circumferential velocity is not low by more than 150 ft/sec, and out-of-plane errors up to  $1^\circ$  velocity offset. A more sophisticated control system should be capable of correcting larger errors and should demonstrate greater economy. A simplified set of guidance commands was tested and worked successfully with virtually no additional fuel consumption.

General analysis of the coplanar launch and rendezvous energy requirements for this case led to the conclusion that the shortest burning time consistent with the size of errors expected from the launch guidance should be used for the best mass ratio, and demonstrated that the penalty in mass ratio for using low thrust and burning times longer than the minimum possible was less than 1 percent.

Langley Research Center,  
National Aeronautics and Space Administration,  
Langley Field, Va., May 19, 1961.

L  
1  
5  
2  
2



## APPENDIX A

EXACT CALCULATIONS FOR FINITE BURNING TIMES AND  
IMPULSIVE TRANSFER VELOCITY REQUIREMENTS

In order to determine the degree of approximation involved in using the simplified equations of motion, trajectories were numerically calculated on the IBM type 704 electronic data processing machine for the terminal stage by using the exact dynamics. The exact equations were written in polar coordinates. These cases were for constant thrust in the circumferential direction, and were run in negative time from the rendezvous condition for burning times of 100, 200, 300, and 400 seconds. Negative thrust was used to drive the ferry to the initial condition from which normal rendezvous could be accomplished. The equations programmed were

$$\ddot{R} = R(\dot{\Omega})^2 - \frac{\gamma}{R^2}$$

$$\ddot{\Omega} = \frac{1}{R} \left( \frac{T_X}{m} - 2\dot{R}\dot{\Omega} \right)$$

$$m = m_0 - \frac{T_X}{c} t$$

$$X = R_S \Omega$$

$$\dot{X} = R_S \dot{\Omega}$$

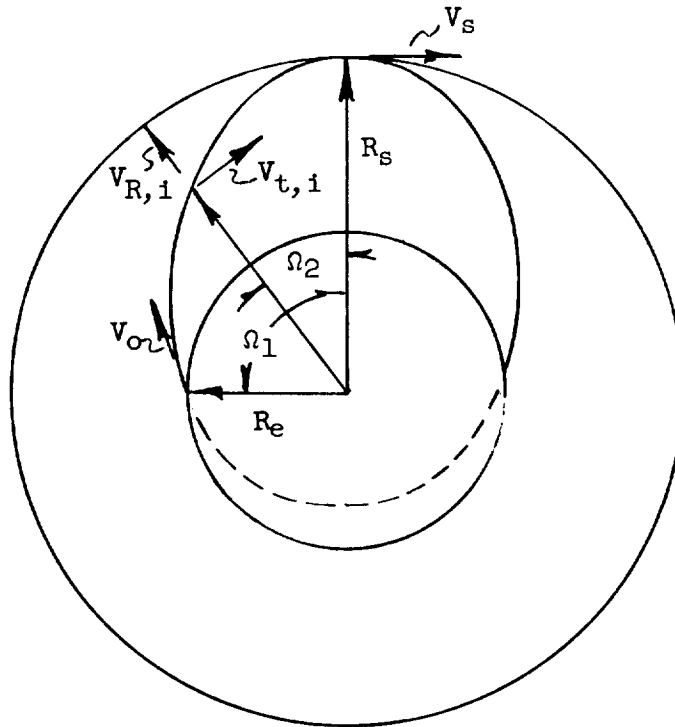
$$Z = R_S - R$$

$$\dot{Z} = -\dot{R}$$

This program was used for a range of thrusts to determine the variation of terminal-stage characteristic velocity with initial circumferential velocity increment to be gained for rendezvous with a station in a 400-nautical-mile circular orbit. Characteristic velocities based on the mass change during these runs were calculated by means of equation (13). Ratios of these characteristic velocities to approximate characteristic velocities were calculated and are plotted against the initial circumferential velocity increment in figure 5.

In order to determine the loss of efficiency with increase in burning time, the initial launch velocity impulse required to establish the

desired terminal-stage initial conditions was calculated where vacuum trajectories were assumed. Empirical relations were developed for the terminal-stage initial conditions from the program described previously. The constraint placed on the launching trajectories for comparison of the various burning times was that the angle of transfer from launch to ignition of the terminal stage should be constant. This constraint was felt to be reasonable, inasmuch as it represented a condition where launch trajectory errors would be the same for each case at initiation. Computations were carried out for assumed circumferential velocity increments at terminal-stage ignition and the results cross-plotted to yield the variation of required launch velocity impulse and of final circumferential velocity increment at ignition with transfer angle. These results are plotted in figure 12(a). The relations used in obtaining these quantities, with  $V_s - V_{t,i}$  given, are (from definitions given in the following sketch):



$$\Omega_T = \Omega_1 - \Omega_2$$

$$V_{R,i} = \frac{V_s}{R_s} (V_s - V_{t,i}) \Delta t$$

$$V_i^2 = V_{t,i}^2 + V_{R,i}^2$$

$$R_i = R_s - \frac{V_s (V_s - V_{t,i}) (\Delta t)^2}{2.95 R_s}$$

$$V_o^2 = 2\gamma \left( \frac{1}{R_e} - \frac{1}{R_i} \right) + V_i^2$$

$$\cos \Omega_1 = \frac{\frac{(R_i V_{t,i})^2}{\gamma R_e} - 1}{\left[ \left( 1 - \frac{R_i V_{t,i}^2}{\gamma} \right)^2 + \left( \frac{R_i V_{t,i} V_{R,i}}{\gamma} \right)^2 \right]^{1/2}}$$

$$\cos \Omega_2 = \frac{\frac{R_i V_{t,i}^2}{\gamma} - 1}{\left[ \left( 1 - \frac{R_i V_{t,i}^2}{\gamma} \right)^2 + \left( \frac{R_i V_{t,i} V_{R,i}}{\gamma} \right)^2 \right]^{1/2}}$$

The expressions for  $V_{R,i}$  and  $R_i$  are empirical, and the remainder are derived from elliptical-orbit equations.

## APPENDIX B

APPLICATION OF WRIGLEY'S PROPORTIONAL NAVIGATION  
TO STEERING IN THE HORIZONTAL PLANE

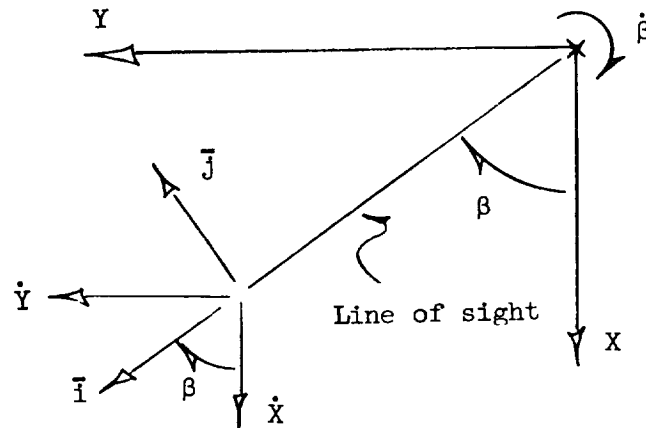
In reference 5, Wrigley proposes a proportional steering scheme whereby the thrust is applied in such a manner that the angular rate of the line of sight is driven to zero. The specification for the thrust acceleration vector is

$$\bar{f}_c = S_{cs}\bar{\omega}_{ls} \times \bar{V}_{c,s} + \bar{l}_v\dot{\bar{V}}_{c,s} + (\bar{\omega}_{I,s} \text{ terms}) \quad (B1)$$

where

$f_c$	thrust per unit mass of commuter
$S_{cs}$	proportionality constant
$\bar{\omega}_{ls}$	rotation of line of sight in space-station coordinates
$\bar{V}_{c,s}$	commuter velocity relative to station
$\bar{l}_v$	unit vector along $\bar{V}_{c,s}$
$\bar{\omega}_{I,s}$	rotation of space station in earth-centered inertial coordinates

The  $\bar{\omega}_{I,s}$  terms will be neglected since they can be shown to be small in comparison to the other terms. If  $\bar{i}$ ,  $\bar{j}$ , and  $\bar{k}$  are defined as unit vectors along the projection of the line of sight in the horizontal plane, the normal in this plane, and the Z-station axis, then the vectors in equation (B1) can be written in terms of these coordinates. Refer to the following sketch:



where

$$\bar{f}_c = \bar{i}f_{ls} + \bar{j}f_n \quad (B2)$$

$$\bar{\omega}_{ls} = \bar{k}\dot{\beta} \quad (B3)$$

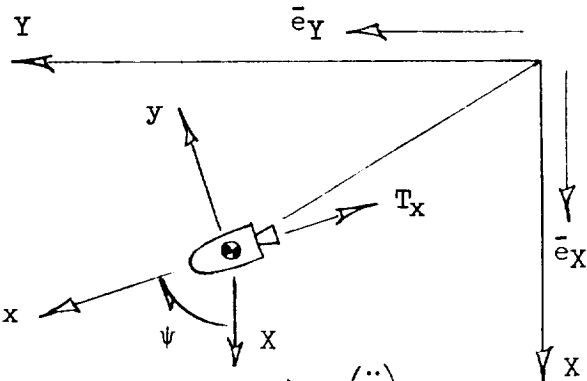
$$\bar{v}_{c,s} = \bar{i}[(v_s - \dot{x})\cos\beta - \dot{y}\sin\beta] - \bar{j}[(v_s - \dot{x})\sin\beta + \dot{y}\cos\beta] \quad (B4)$$

$$\bar{l}_v = \frac{\bar{v}_{c,s}}{\bar{v}_{c,s}} = \bar{i} \frac{[(v_s - \dot{x})\cos\beta - \dot{y}\sin\beta]}{[(v_s - \dot{x})^2 + \dot{y}^2]^{1/2}} - \bar{j} \frac{[(v_s - \dot{x})\sin\beta + \dot{y}\cos\beta]}{[(v_s - \dot{x})^2 + \dot{y}^2]^{1/2}} \quad (B5)$$

$$\dot{v}_{c,s} = \frac{\dot{y}\ddot{y} - (v_s - \dot{x})\ddot{x}}{[(v_s - \dot{x})^2 + \dot{y}^2]^{1/2}} \quad (B6)$$

and the  $\dot{z}$ -velocity and  $z$ -displacements are neglected. The accelerations  $\ddot{x}$  and  $\ddot{y}$  can be written in terms of the thrust and heading angle  $\psi$ .

A second set of unit vectors  $\bar{e}_x, \bar{e}_y$  along the  $X, Y$  axes is defined for this purpose in the following sketch, and  $\dot{z}$ -velocities and  $z$ -displacements are again neglected.



$$\begin{aligned} \frac{\bar{T}_X}{m} &= \frac{T_X}{m} (\bar{e}_X \cos \psi + \bar{e}_Y \sin \psi) = (\ddot{\bar{R}})_I \\ &= (\ddot{\bar{R}})_s + 2\bar{\omega}_{I,s} \times (\dot{\bar{R}})_s + \dot{\bar{\omega}}_{I,s} \times \bar{R} + \bar{\omega}_{I,s} \times (\bar{\omega}_{I,s} \times \bar{R}) \end{aligned}$$

where

$$(\ddot{\bar{R}})_s = \bar{e}_X \ddot{X} + \bar{e}_Y \ddot{Y}$$

$$(\dot{\bar{R}})_s = \bar{e}_X \dot{X} + \bar{e}_Y \dot{Y}$$

$$\bar{R} = \bar{e}_X X + \bar{e}_Y Y + \bar{k} R_s$$

$$\bar{\omega}_{I,s} = -\bar{e}_Y \omega_{I,s}$$

$$\dot{\bar{\omega}}_{I,s} = 0$$

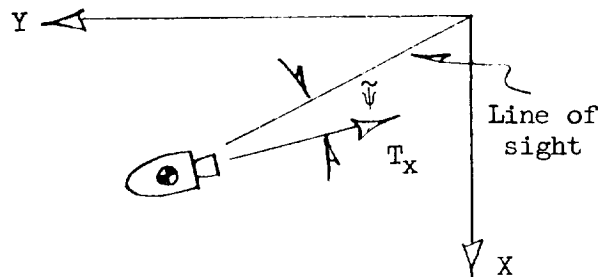
$$\frac{T_X}{m} (\bar{e}_X \cos \psi + \bar{e}_Y \sin \psi) = \bar{e}_X \ddot{X} + \bar{e}_Y \ddot{Y} + 2\omega_{I,s} (\bar{k} \dot{X}) - \omega_{I,s}^2 (\bar{e}_X X + \bar{k} R_s)$$

Equate vector components and solve for  $\ddot{X}$  and  $\ddot{Y}$  to obtain

$$\ddot{X} = \frac{T_X}{m} \cos \psi - \omega_{I,s}^2 X$$

$$\ddot{Y} = \frac{T_X}{m} \sin \psi$$

The  $\omega_{I,s}^2 x$  term in  $\ddot{X}$  is negligible in view of previous assumptions. Substitute the identity  $\psi = \beta + \tilde{\psi}$  where  $\tilde{\psi}$  is a command tilt angle with respect to the line of sight as indicated in the following sketch:



and

$$\ddot{X} = \frac{T_x}{m} (\cos \tilde{\psi} \cos \beta - \sin \tilde{\psi} \sin \beta) \quad (B7)$$

$$\ddot{Y} = \frac{T_x}{m} (\sin \tilde{\psi} \cos \beta + \cos \tilde{\psi} \sin \beta) \quad (B8)$$

Substitute equations (B7) and (B8) into equation (B6).

$$\dot{V}_{c,s} = \frac{T_x}{m} \frac{[\dot{Y} \cos \beta + (V_s - \dot{X}) \sin \beta] \sin \tilde{\psi} + [\dot{Y} \sin \beta - (V_s - \dot{X}) \cos \beta] \cos \tilde{\psi}}{[(V_s - \dot{X})^2 + \dot{Y}^2]^{1/2}} \quad (B9)$$

Substitute equations (B2), (B3), (B4), (B5), and (B9) into equation (B1) and equate components of the unit vectors to yield

$$f_{ls} = \left[ S_{cs} \dot{\beta} + \frac{T_x}{m} \sin \tilde{\psi} \frac{(V_s - \dot{X}) \cos \beta - \dot{Y} \sin \beta}{(V_s - \dot{X})^2 + \dot{Y}^2} \right] [(V_s - \dot{X}) \sin \beta + \dot{Y} \cos \beta] - \frac{T_x}{m} \sin \tilde{\psi} \frac{[(V_s - \dot{X}) \cos \beta - \dot{Y} \sin \beta]^2}{(V_s - \dot{X})^2 + \dot{Y}^2} \quad (B10)$$

$$f_n = \left[ S_{cs} \dot{\beta} + \frac{T_x}{m} \cos \tilde{\psi} \frac{(V_s - \dot{X}) \sin \beta + \dot{Y} \cos \beta}{(V_s - \dot{X})^2 + \dot{Y}^2} \right] [(V_s - \dot{X}) \cos \beta - \dot{Y} \sin \beta] \\ - \frac{T_x}{m} \sin \tilde{\psi} \frac{[(V_s - \dot{X}) \sin \beta + \dot{Y} \cos \beta]^2}{(V_s - \dot{X})^2 + \dot{Y}^2} \quad (B11)$$

The longitudinal guidance system will command the value for  $T_x/m$ .  
Tilt the thrust vector away from the line of sight by the angle  $\tilde{\psi}$  to  
generate the required  $f_n$ , and assume

$$\sin \tilde{\psi} \approx \tilde{\psi} \quad \cos \tilde{\psi} \approx 1$$

then

$$f_n \approx \frac{T_x}{m} \tilde{\psi}$$

and

$$\tilde{\psi} = \frac{1}{\frac{T_x}{m}} \left[ S_{cs} \dot{\beta} + \frac{T_x}{m} \frac{(V_s - \dot{X}) \sin \beta + \dot{Y} \cos \beta}{(V_s - \dot{X})^2 + \dot{Y}^2} \right] \frac{(V_s - \dot{X}) \cos \beta - \dot{Y} \sin \beta}{1 + \frac{[(V_s - \dot{X}) \sin \beta + \dot{Y} \cos \beta]^2}{(V_s - \dot{X})^2 + \dot{Y}^2}} \quad (B12)$$

Now introduce the following expressions derived from equations (10)  
and (C6):

$$\frac{T_x}{m} \approx \frac{(V_s - \dot{X})^2 + \dot{Y}^2}{2[(X - V_{st})^2 + Y^2]^{1/2}} \quad (B13)$$

$$\dot{\beta} [(X - V_{st})^2 + Y^2]^{1/2} = (V_s - \dot{X}) \sin \beta + \dot{Y} \cos \beta \quad (B14)$$

Substituting these expressions into equation (B12) yields

$$\tilde{\psi} = \frac{\dot{\beta}}{\frac{T_x}{m}} \frac{\left( S_{cs} + \frac{1}{2} \right) [(V_s - \dot{X}) \cos \beta - \dot{Y} \sin \beta]}{1 + \dot{\beta}^2 \frac{(X - V_{st})^2 + Y^2}{(V_s - \dot{X})^2 + \dot{Y}^2}} \quad (B15)$$



For the conditions considered in this report, the  $\dot{\beta}^2$  term in the denominator is negligible. Moreover the guidance system drives  $\dot{\beta}$  toward zero. Neglect this term and define

$$K_{\dot{\beta}} \equiv S_{cs} + \frac{1}{2}$$

to yield the final  $\tilde{\psi}$  expression, which is

$$\tilde{\psi} = \frac{K_{\dot{\beta}} \dot{\beta}}{\frac{T_x}{m}} \left[ (v_s - \dot{x}) \cos \beta - \dot{y} \sin \beta \right] \quad (\text{B16})$$

Now inspect the thrust required along the line of sight. Introducing equations (B14) and (B16) into equation (B10) and assuming  $\tilde{\psi}$  to be small, as before, yields

$$f_{ls} = K_{\dot{\beta}} \dot{\beta}^2 \left\{ 1 - \frac{1}{2K_{\dot{\beta}}} + \frac{\left[ (v_s - \dot{x}) \cos \beta - \dot{y} \sin \beta \right]^2}{(v_s - \dot{x})^2 + \dot{y}^2} \right\} \left[ (x - v_s t)^2 + y^2 \right]^{1/2} \\ - \frac{T_x}{m} \frac{\left[ (v_s - \dot{x}) \cos \beta - \dot{y} \sin \beta \right]^2}{(v_s - \dot{x})^2 + \dot{y}^2} \quad (\text{B17})$$

Again neglect  $\dot{\beta}^2$ ; the following result is apparent:

$$|f_{ls}| \leq \frac{T_x}{m}$$

and the required thrust is directed toward the space station. Accordingly, no lateral correction was introduced and the longitudinal system was allowed to control  $T_x/m$ .

## APPENDIX C

INTRODUCTION OF MEASURED VARIABLES INTO  
GUIDANCE COMMAND EQUATIONS

Express the variables measured by the rendezvous guidance system in terms of the rectangular-coordinate system geometry. (See fig. 5.)

$$\rho = [(X - v_{st})^2 + Y^2 + Z^2]^{1/2} \quad (C1)$$

$$\dot{\rho} = \frac{(X - v_{st})(\dot{X} - v_s) + Y\dot{Y} + Z\dot{Z}}{\rho} \quad (C2)$$

$$\alpha = \sin^{-1}\left(\frac{Z}{\rho}\right) \quad (C3)$$

$$\dot{\alpha} = \frac{\dot{Z} - Z\left(\frac{\dot{\rho}}{\rho}\right)}{(\rho^2 - Z^2)^{1/2}} \quad (C4)$$

$$\beta = \tan^{-1}\left(\frac{Y}{X - v_{st}}\right) \quad (C5)$$

$$\dot{\beta} = \frac{\dot{Y}(X - v_{st}) - Y(\dot{X} - v_s)}{(X - v_{st})^2 + Y^2} \quad (C6)$$

For simplicity, consider that each measurement is made with the station at the origin of a new set of coordinates and  $t = 0$ , and use the measured variables with a subscript 0 to denote this.

It is necessary to restate equations (10) to (12) in terms of the variables sensed by the rendezvous guidance system. Express  $V_s - \dot{X}_0$  and  $X_0$  in terms of the measured variables  $\rho$ ,  $\dot{\rho}$ , and  $\alpha$ . The quantities  $Y$  and  $\dot{Y}$  must be neglected, since it is not possible to isolate these quantities in the proposed measurement scheme.

$$V_s - \dot{X}_O = \rho \dot{\alpha} \sin \alpha - \dot{\rho} \cos \alpha \quad (C7)$$

$$X_O = \rho \cos \alpha \quad (C8)$$

Represent the sine and cosine functions by their respective series. Since maximum values of elevation angle are expected to be less than 0.3 radian, truncate these series after the cubic power term

$$\sin \alpha \approx \alpha - \frac{\alpha^3}{6} \quad (C9)$$

$$\cos \alpha \approx 1 - \frac{\alpha^2}{2} \quad (C10)$$

Note that the sine and cosine terms can be retained and supplied to the guidance computer by a resolver. It is felt that supplying the elevation angle directly would result in both a weight saving and an increased reliability. Two approximations can be used to help weight terms in arriving at final expressions. These approximations are

$$\dot{\alpha} \approx - \frac{\alpha}{t_r} \quad (C11)$$

$$\rho \approx - \frac{\dot{\rho} t_r}{2} \quad (C12)$$

Now equations (C7) to (C12) can be substituted into equations (10), (11), and (12). Retaining terms consistent with previous approximations yields

$$Z_{com} = -\rho^2 \left[ A_1 (1 - \alpha^2) + \frac{A_2}{\dot{\rho}} \right] \quad (C13)$$

$$\dot{Z}_{com} = -\rho \left[ A_3 \left( 1 - \frac{\alpha^2}{2} \right) + A_4 \dot{\rho} \right] \quad (C14)$$

where

$$A_1 = \frac{V_s}{9cR_s} \left( 1 + \frac{3c}{V_s} \right)$$

$$A_2 = \frac{4V_s}{3R_s}$$

$$A_3 = \frac{2V_s}{R_s}$$

$$A_4 = \frac{2}{3R_s}$$

and

$$\left(\frac{T_x}{m}\right)_{\text{com}} = \frac{\dot{\rho}^2}{2\rho} \left(1 + \frac{\dot{\rho}}{3c} - \frac{2\rho\dot{\alpha}\alpha}{\dot{\rho}}\right) \quad (\text{C15})$$

Use similar means to introduce measured variables into the lateral-control command equation, which is

$$\tilde{\psi}_{\text{com}} = \frac{K_{\beta}\dot{\beta}}{\frac{T_x}{m}} \left[ (V_s - \dot{x}_o) \cos \beta - \dot{y}_o \sin \beta \right] \quad (\text{C16})$$

Note that  $\sin \beta_o$ ,  $\cos \beta_o$ , and  $\dot{\rho}$  can be expressed

$$\sin \beta_o = \frac{y_o}{\rho \cos \alpha} \quad (\text{C17})$$

$$\cos \beta_o = \frac{x_o}{\rho \cos \alpha} \quad (\text{C18})$$

$$\dot{\rho} = \frac{(\dot{x}_o - v_s)x_o + y_o\dot{y}_o + z_o\dot{z}_o}{\rho} \quad (\text{C19})$$

Substituting equations (C17) to (C19) into equation (C16) gives

$$\tilde{\psi}_{\text{com}} = \frac{K_{\beta}\dot{\beta}}{\frac{T_x}{m}} (\dot{\rho} \cos \alpha - \rho\dot{\alpha} \sin \alpha) \quad (\text{C20})$$

Now the same means of weighting terms used before can be employed with the additional consideration that the lateral and longitudinal systems

should be divorced as much as possible, and the rather simple control relationship results

$$\tilde{\psi}_{\text{com}} = \frac{K_{\dot{\beta}} \dot{\beta}}{\frac{T_X}{m}} \dot{\rho} \quad (\text{C21})$$

L  
1  
5  
2  
2

## APPENDIX D

## STABILITY ANALYSIS OF LONGITUDINAL AND LATERAL CONTROLS

## Longitudinal Controller

In this appendix, the notation and techniques will be drawn principally from reference 10. By referring to figure 6, write transfer functions for the various blocks in the diagram. If the vehicle dynamics are linearized

$$T_z = K_\delta \delta_y$$

$$M_y = -d_x K_\delta \delta_y$$

$$\dot{q} = \frac{M_y}{I_y} = - \frac{d_x K_\delta \delta_y}{I_y}$$

$$\ddot{z} = \frac{T_z}{m} \cos \theta - \frac{T_x}{m} \sin \theta$$

$$\approx \frac{T_z}{m} - \frac{T_x}{m} \theta$$

Now taking the Laplace transforms of these variables and writing them in transfer-function form yields

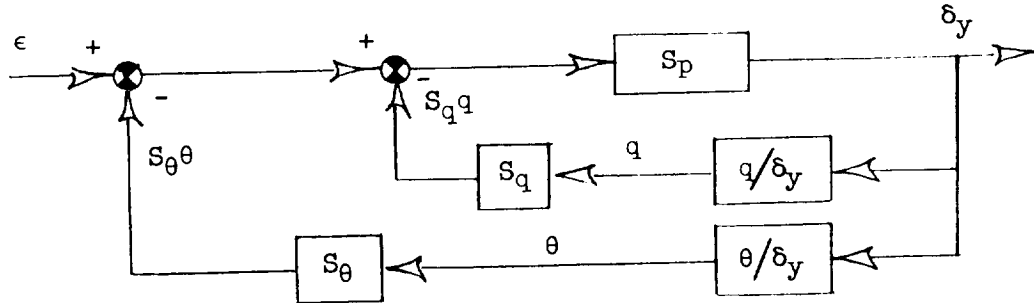
$$\frac{q}{\delta_y} = - \frac{d_x K_\delta}{I_y} \frac{1}{\lambda}$$

$$\frac{\theta}{\delta_y} = - \frac{d_x K_\delta}{I_y} \frac{1}{\lambda^2}$$

$$\frac{z}{\delta_y} = \left( \frac{K_\delta}{m} + \frac{T_x}{m} \frac{d_x K_\delta}{I_y} \frac{1}{\lambda^2} \right) \frac{1}{\lambda^2}$$

$$= \frac{K_\delta d_x T_x}{m I_y} \left( \frac{I_y}{d_x T_x} \lambda^2 + 1 \right) \frac{1}{\lambda^4}$$

Consider the attitude control loop shown in the following diagram:



The open-loop performance function for the inner loop is

$$\begin{aligned} [PF]_{ol} &= S_p \left( - \frac{d_x K_\delta}{I_y} \right) \frac{1}{\lambda} S_q \\ &= - \frac{S_p S_q d_x K_\delta}{I_y} \frac{1}{\lambda} \end{aligned}$$

Let

$$\tau \equiv - \frac{I_y}{S_p S_q d_x K_\delta}$$

then

$$[PF]_{ol} = \frac{1}{\tau \lambda}$$

Closing this loop gives

$$\begin{aligned} [PF]_{cl} &= \frac{\frac{1}{\tau \lambda}}{1 + \frac{1}{\tau \lambda}} \\ &= \frac{1}{\tau \lambda + 1} \end{aligned}$$

and writing the overall loop transfer function gives

$$\frac{\delta_y}{\Delta} = - \frac{I_y}{S_q d_x K_\delta} \frac{\lambda}{\tau \lambda + 1}$$

The open-loop performance function for the outer loop is

$$\begin{aligned} [PF]_{ol} &= - \frac{I_y}{S_q d_x K_\delta} \frac{\lambda}{\tau\lambda + 1} \left( - \frac{d_x K_\delta}{I_y} \right) \frac{1}{\lambda^2} S_\theta \\ &= \frac{S_\theta}{S_q} \frac{1}{\lambda(\tau\lambda + 1)} \end{aligned}$$

Closing this loop gives

$$\begin{aligned} [PF]_{cl} &= \frac{\frac{S_\theta}{S_q} \frac{1}{\lambda(\tau\lambda + 1)}}{1 + \frac{S_\theta}{S_q} \frac{1}{\lambda(\tau\lambda + 1)}} \\ &= \frac{1}{\frac{\tau S_q}{S_\theta} \lambda^2 + \frac{S_q}{S_\theta} \lambda + 1} \\ &= \frac{1}{\left(\frac{\lambda}{\omega}\right)^2 + \frac{2\xi\lambda}{\omega} + 1} \end{aligned}$$

where

$$\begin{aligned} \omega^2 &= - \frac{S_\theta S_p d_x K_\delta}{I_y} \\ \frac{2\xi}{\omega} &= \frac{S_q}{S_\theta} \end{aligned}$$

and writing the total attitude loop transfer function gives

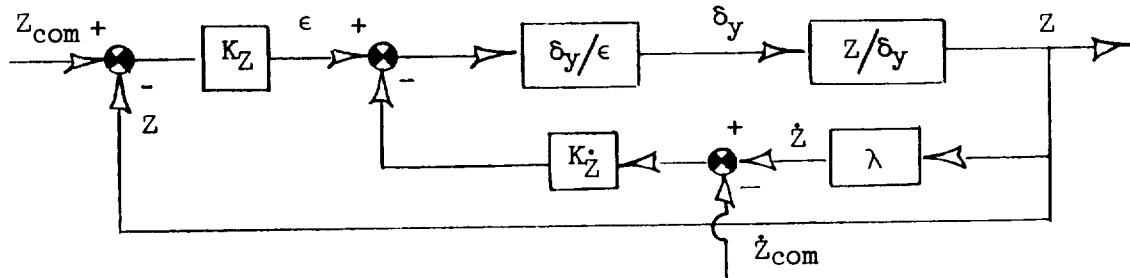
$$\frac{\delta_y}{\epsilon} = - \frac{I_y}{S_\theta d_x K_\delta} \frac{\lambda^2}{\left(\frac{\lambda}{\omega}\right)^2 + \frac{2\xi\lambda}{\omega} + 1}$$

It is apparent that this simplified inner loop is of second order and has dynamics which may be arbitrarily selected by the designer.

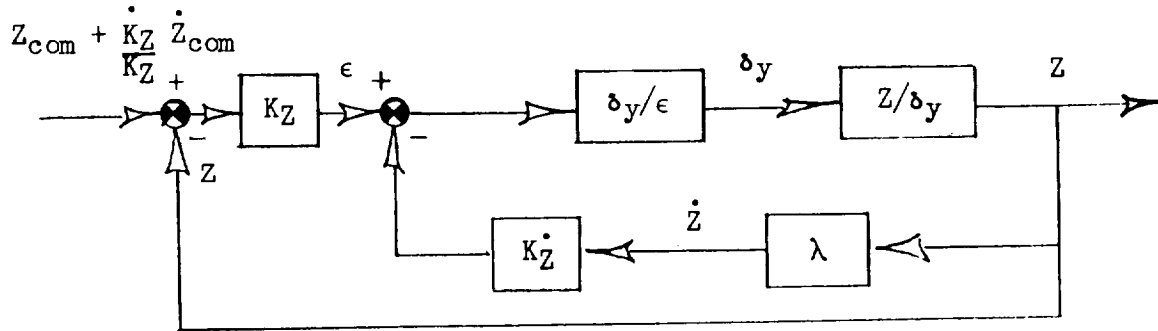
L  
1  
5  
2  
2



Now consider the total control loop illustrated in the following diagram:



The  $\dot{Z}_{com}$  can be combined with  $Z_{com}$ , with the reasoning that the nonlinearities in this quantity are gravitational in origin and may be neglected if gravity is neglected. In fact, these commands serve to make the control system detect a nearly gravity-free environment and, indeed, to make the linearized analysis a good representation of the system's real performance. The resulting block diagram is



The open-loop performance function for the inner loop of the preceding sketch is

$$\begin{aligned}
 [PF]_{ol} &= - \frac{I_y}{S_{\theta} d_x K_{\delta}} \frac{\lambda^2}{\left(\frac{\lambda}{\omega}\right)^2 + \frac{2\zeta\lambda}{\omega} + 1} \frac{K_{\delta} d_x T_x}{m I_y} \left( \frac{I_y}{d_x T_x} \lambda^2 + 1 \right) \frac{\lambda K_Z}{\lambda^4} \\
 &= - \frac{K_Z T_x}{S_{\theta} m} \frac{\frac{I_y \lambda^2}{d_x T_x} + 1}{\lambda \left[ \left(\frac{\lambda}{\omega}\right)^2 + \frac{2\zeta\lambda}{\omega} + 1 \right]}
 \end{aligned}$$

Closing this loop will yield a third-order characteristic equation. The result will be of the form

$$\frac{Z}{\epsilon} = \frac{\frac{I_y \lambda^2}{d_x T_x} + 1}{K_Z \lambda (\tau_1 \lambda + 1) \left[ \left( \frac{\lambda}{\omega_1} \right)^2 + \frac{2\zeta_1 \lambda}{\omega_1} + 1 \right]}$$

where  $\tau_1$ ,  $\zeta_1$ , and  $\omega_1$  can be determined by root-locus techniques.

Again this function can be carried into the outer loop, and the open-loop performance function determined

$$[PF]_{ol} = \frac{K_Z}{K_Z} \frac{\frac{I_y \lambda^2}{d_x T_x} + 1}{\lambda (\tau_1 \lambda + 1) \left[ \left( \frac{\lambda}{\omega_1} \right)^2 + \frac{2\zeta_1 \lambda}{\omega_1} + 1 \right]}$$

For the guidance-problem studies in this paper, the attitude loop was arbitrarily set up for  $\zeta = 0.7$  and  $\omega = 1.414$  radians. This condition yielded the following system constants where an arbitrary value of 300 was selected for  $S_p K_\delta$  and

$$S_\theta = -5$$

$$S_q = -5$$

Note that  $S_p$  is redundant.

The root locus for the inner Z-loop appears in figure 14 with the closed-loop roots selected for the 200- and 400-second burning times. These roots were carried to the outer loop plot, and the two corresponding loci also appear in figure 14. The final Z-loop gains corresponding to the open-loop sensitivities from the root loci were as follows:

	200-second case	400-second case
$K_Z$ . . . . .	0.122	0.18
$K_Z$ . . . . .	0.0091	0.008

Note that the response for these gains is rather slow. These gains were purposely selected to allow the system to operate on very large errors before exceeding the tilt-angle limit, and since a relatively long time is available for correcting errors.

### Lateral Controller

Refer to figure 6 and note that in this section the object is to establish the commanded tilt angle  $\tilde{\psi}$ . Linearizing the lateral dynamic equations yields

$$T_y = K_{\delta} \delta_z$$

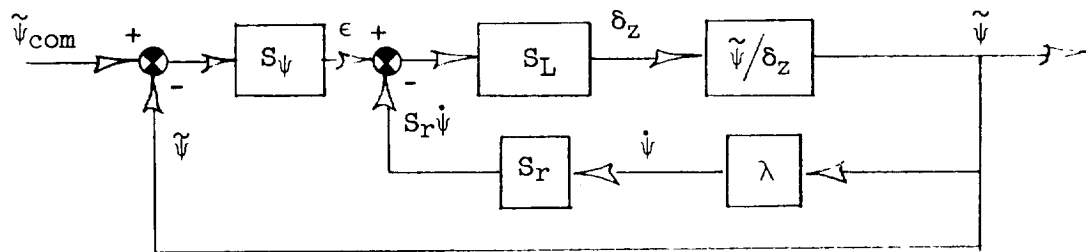
$$M_z = d_x K_{\delta} \delta_z$$

$$\dot{r} = \frac{M_z}{I_z} = \frac{K_{\delta} d_x}{I_z} \delta_z$$

Taking the Laplace transform yields

$$\frac{\tilde{\psi}}{\delta_z} = \frac{K_{\delta} d_x}{I_z} \frac{1}{\lambda^2}$$

Consider the inner loop shown in the following sketch



and write the open-loop performance function

$$[PF]_{ol} = S_L \frac{K_{\delta} d_x}{I_z} \frac{1}{\lambda^2} \lambda S_r$$

$$= \frac{S_L S_r K_{\delta} d_x}{I_z} \frac{1}{\lambda}$$

where

$$\tau_2 \equiv \frac{I_z}{S_L K_{\delta} d_x S_r}$$

Then

$$[PF]_{ol} = \frac{1}{\tau_2 \lambda}$$

If this loop is closed

$$[PF]_{cl} = \frac{1}{\tau_2 \lambda + 1}$$

and the desired transfer function can be written

$$\frac{\tilde{\psi}}{\epsilon} = \frac{1}{S_r \lambda} \frac{1}{\tau_2 \lambda + 1}$$

Now follow the same procedure for the outer loop to obtain the following equations:

$$[PF]_{ol} = \frac{S_\psi}{S_r} \frac{1}{\lambda(\tau_2 \lambda + 1)}$$

$$\frac{\tilde{\psi}}{\tilde{\psi}_{com}} = \frac{1}{\left(\frac{\lambda}{\omega_2}\right)^2 + \frac{2\zeta_2 \lambda}{\omega_2^2} + 1}$$

where

$$\omega_2^2 = \frac{S_\psi S_L K_\delta d_x}{I_z}$$

$$\frac{2\zeta_2}{\omega_2} = \frac{S_r}{S_\psi}$$

The dynamics of this system are again at the disposal of the designer. The following gains, corresponding to  $\zeta_2 = 0.7$  and  $\omega_2 = 1.428$ , were selected with  $S_L$  being redundant:

$$S_L K_\delta = 300$$

$$S_\psi = 5$$

$$S_r = 2.5$$

## APPENDIX E

## EQUATIONS OF MOTION FOR NUMERICAL SOLUTION

The equations of motion for the rendezvous vehicle were written in Eulerian axes centered at the vehicle center of gravity. (See fig. 1.) Since the vehicle was assumed to be roll stabilized to the horizontal plane sensed by the horizon seeker, the third Euler angle  $\phi$  rotation was suppressed. This has the effect of constraining the Y-axis to the horizontal plane and requires the following substitution to account for rotation about the X-axis as a result of this constraint:

$$\dot{\phi} = p - r \tan \theta = 0$$

$$p = r \tan \theta$$

The motion of the vehicle was referred to a rectangular X,Y,Z axis system with origin at the space station's location at time zero. Additional auxiliary relations were required to calculate the measured variables and to represent the control system; these relations are listed in appropriate groups.

Dynamics:

$$\dot{u} = rv - qw + \frac{T_x}{m} - G \sin \theta$$

$$\dot{v} = -r(u + w \tan \theta) + \frac{T_y}{m}$$

$$\dot{w} = rv \tan \theta + qu + \frac{T_z}{m} + G \cos \theta$$

$$\dot{q} = r^2 \tan \theta \left( \frac{I_x - I_z}{I_y} \right) + \frac{M_y}{I_y}$$

$$\dot{r} = qr \tan \theta \left( \frac{I_y - I_x}{I_z} \right) + \frac{M_z}{I_z}$$

$$\dot{\theta} = q$$

$$\dot{\psi} = \frac{r}{\cos \theta}$$

$$G = \frac{\gamma}{(R_s - z)^2} - \frac{\dot{x}^2 + \dot{y}^2}{R_s - z}$$

Varying mass parameters:

$$\dot{m} = - \frac{T_x}{c}$$

$$d_x = d_{x,0} + d_{x,1}t$$

$$I_x = I_{x,0} + I_{x,1}t$$

$$I_y = I_{y,0} + I_{y,1}t + I_{y,2}t^2 + I_{y,3}t^3$$

$$I_z = I_{z,0} + I_{z,1}t + I_{z,2}t^2 + I_{z,3}t^3$$

Geometrical relations:

$$\dot{X} = u \cos \psi \cos \theta - v \sin \psi + w \cos \psi \sin \theta$$

$$\dot{Y} = u \sin \psi \cos \theta + v \cos \psi + w \sin \psi \sin \theta$$

$$\dot{Z} = -u \sin \theta + w \cos \theta$$

Measured variables:

$$\rho = [(X - V_{st})^2 + Y^2 + Z^2]^{1/2}$$

$$\dot{\rho} = \frac{(X - V_{st})(\dot{X} - V_s) + Y\dot{Y} + Z\dot{Z}}{\rho}$$

$$\alpha = \sin^{-1}\left(\frac{Z}{\rho}\right)$$

$$\dot{\alpha} = \frac{\dot{Z} - Z\left(\frac{\dot{\rho}}{\rho}\right)}{(\rho^2 - Z^2)^{1/2}}$$

$$\beta = \tan^{-1}\left(\frac{Y}{X - V_{st}}\right)$$

$$\dot{\beta} = \frac{\dot{Y}(X - V_{st}) - Y(\dot{X} - V_s)}{(X - V_{st})^2 + Y^2}$$

$$\tilde{\psi} = \psi - \beta$$

Control forces and moments:

$$\frac{T_y}{m} = \frac{K_\delta}{m} \delta_z$$

$$\frac{T_z}{m} = \frac{K_\delta}{m} \delta_y$$

$$\frac{M_y}{I_y} = - \frac{K_{\delta^d x}}{I_y} \delta_y$$

$$\frac{M_z}{I_z} = \frac{K_{\delta^d x}}{I_z} \delta_z$$

Guidance commands:

$$\left( \frac{T_x}{m} \right)_{\text{com}} = \frac{\dot{\rho}^2}{2\rho} \left( 1 + \frac{\dot{\rho}}{3c} - \frac{2\rho}{\dot{\rho}} \alpha \dot{\alpha} \right)$$

$$z_{\text{com}} = -\rho^2 \left[ A_1 (1 - \alpha^2) + \frac{A_2}{\dot{\rho}} \right]$$

$$\dot{z}_{\text{com}} = -\rho \left[ A_3 \left( 1 - \frac{\alpha^2}{2} \right) + A_4 \dot{\rho} \right]$$

$$\tilde{\psi}_{\text{com}} = \frac{K_{\dot{\beta}} \dot{\beta} \dot{\rho}}{\frac{T_x}{m}}$$

Feedback variables:

$$z_{\text{meas}} = \rho \alpha \left( 1 - \frac{\alpha^2}{6} \right)$$

$$\dot{z}_{\text{meas}} = \dot{\rho} \alpha \left( 1 - \frac{\alpha^2}{6} \right) + \rho \dot{\alpha} \left( 1 - \frac{\alpha^2}{2} \right)$$

Fuel consumption relations:

$$\eta_x = \int_0^t |T_x| dt$$

$$\eta_y = \int_0^t |T_y| dt$$

$$\eta_z = \int_0^t |T_z| dt$$

where  $| \quad |$  denotes absolute value.

The physical constants employed were derived by scaling the Mercury capsule up to a 300-slug vehicle and elongating it to about 18 feet. The control constants appear in appendix D, and the remaining physical constants are tabulated as follows:

$R_s$ , ft . . . . .	23,333,380	
$V_s$ , ft/sec <sup>2</sup> . . . . .	24,563.66	
$\gamma$ , ft <sup>3</sup> /sec <sup>2</sup> . . . . .	$1.4078741 \times 10^{16}$	
$m_0$ , slugs . . . . .	300	
$I_{x,0}$ , slug-ft <sup>2</sup> . . . . .	1,800	
$I_{y,0}$ , slug-ft <sup>2</sup> . . . . .	7,500	
$I_{z,0}$ , slug-ft <sup>2</sup> . . . . .	7,500	
$d_{x,0}$ , ft . . . . .	10	
$c$ , ft/sec . . . . .	10,000	
	200-second case	400-second case
$d_{x,1}$ , ft/sec . . . . .	-0.005	-0.0025
$I_{x,1}$ , slug-ft <sup>2</sup> /sec . . . . .	-1.225	-0.6125
$I_{y,1}$ , slug-ft <sup>2</sup> /sec . . . . .	-7.5	-3.75
$I_{z,1}$ , slug-ft <sup>2</sup> /sec . . . . .	-7.5	-3.75
$I_{y,2}$ , slug-ft <sup>2</sup> /sec <sup>2</sup> . . . . .	$-0.5 \times 10^{-2}$	$-0.125 \times 10^{-2}$
$I_{z,2}$ , slug-ft <sup>2</sup> /sec <sup>2</sup> . . . . .	$-0.5 \times 10^{-2}$	$-0.125 \times 10^{-2}$
$I_{y,3}$ , slug-ft <sup>2</sup> /sec <sup>3</sup> . . . . .	$-0.5 \times 10^{-5}$	$-0.625 \times 10^{-6}$
$I_{z,3}$ , slug-ft <sup>2</sup> /sec <sup>3</sup> . . . . .	$-0.5 \times 10^{-5}$	$-0.625 \times 10^{-6}$



## REFERENCES

1. Spradlin, Louis W.: Terminal Guidance for Satellite Rendezvous. M.S. Thesis, M.I.T., 1960.
2. Roberson, Robert E.: Path Control for Satellite Rendezvous. Advances in Astronautical Sciences, vol. 6, The Macmillan Co., 1961, pp. 192-228.
3. Clohessy, W. H., and Wiltshire, R. S.: Terminal Guidance System for Satellite Rendezvous. Jour. Aerospace Sci., vol. 27, no. 9, Sept. 1960, pp. 653-658, 674.
4. Wolowicz, Chester H., Drake, Hubert M., and Videan, Edward N.: Simulator Investigation of Controls and Display Required for Terminal Phase of Coplanar Orbital Rendezvous. NASA TN D-511, 1960.
5. Wrigley, Walter: Performance of a Linear Accelerometer. Vol. 1 - Notes for a Special Summer Program in Orbital and Satellite Vehicles, ch. 9, Dept. Aero. Eng., M.I.T., Aug. 6-17, 1956, pp. 9-1 - 9-19.
6. Bird, John D., and Thomas, David F., Jr.: A Two-Impulse Plan for Performing Rendezvous on a Once-a-Day Basis. NASA TN D-437, 1960.
7. Kalensher, B. E.: Maximum Energy Thrust Attitude Program. Tech. Release No. 34-85 (Contract NASw-6), Jet Propulsion Lab., C.I.T., May 27, 1960.
8. Hickerson, Frederick R., and Cardullo, Mario W.: Variable Thrust Rocket Engines. [Preprint] 1264-60, American Rocket Soc., July 1960.
9. Schmidt, Stanley F., and Harper, Eleanor V.: The Design of Feedback Control Systems Containing a Saturation Type Nonlinearity. NASA TN D-324, 1960.
10. Draper, Charles Stark, McKay, Walter, and Lees, Sidney: Instrument Engineering. Vol. II - Methods for Associating Mathematical Solutions With Common Forms. McGraw-Hill Book Co., Inc., 1953.

TABLE I.- NOMINAL INITIAL CONDITIONS

(a) 200-second burning time

$\sigma$ , deg . . . . .	0	1	2
$X_0$ , ft . . . . .	135,425	129,525	115,841
$Y_0$ , ft . . . . .	0	39,537	70,149
$Z_0$ , ft . . . . .	18,960	18,097	16,094
$u_0$ , ft/sec . . . . .	22,239	22,104	19,446
$v_0$ , ft/sec . . . . .	0	-7,171	-12,492
$w_0$ , ft/sec . . . . .	-280	-280	-280
$\psi_0$ , radians . . . . .	0	0.2963	0.5445

(b) 400-second burning time

$\sigma$ , deg . . . . .	0	1	2
$X_0$ , ft . . . . .	239,619	226,424	197,563
$Y_0$ , ft . . . . .	0	78,420	135,596
$Z_0$ , ft . . . . .	67,214	63,000	54,553
$u_0$ , ft/sec . . . . .	23,389	21,964	18,810
$v_0$ , ft/sec . . . . .	0	-8,039	-13,900
$w_0$ , ft/sec . . . . .	-496	-495	-496
$\psi_0$ , radians . . . . .	0	0.3334	0.6015

L  
1  
5  
2  
2

TABLE II.- COMPARISON OF REQUIRED CHARACTERISTIC VELOCITY  
FOR NORMAL AND SIMPLIFIED GUIDANCE RELATIONS

Error	Characteristic velocity, $\Delta V$	
	For normal guidance relations	For simplified guidance relations
$\sigma = 0^\circ$		
Nominal	1,325.00	1,325.55
$\Delta X = 25,000$	1,499.48	1,505.23
$\Delta X = -25,000$	1,471.23	1,475.77
$\Delta Z = 7,000$	1,498.31	1,502.82
$\Delta Z = -7,000$	1,484.41	1,491.89
$\Delta \dot{X} = -400$	1,842.02	1,844.31
$\Delta \dot{X} = 300$	1,156.99	1,163.67
$\Delta \dot{Z} = 180$	1,508.88	1,507.67
$\Delta \dot{Z} = -200$	1,504.79	1,505.01
$\sigma = 1^\circ$		
Nominal	1,389.45	1,389.72
$\Delta Y = -20,000$	1,445.68	1,438.60
$\Delta Y = 20,000$	1,454.63	1,452.21
$\sigma = 2^\circ$		
Nominal	1,566.82	1,567.75
$\Delta Y = -20,000$	1,647.57	1,658.38
$\Delta Y = 20,000$	1,667.33	1,656.05

L  
1  
5  
2  
2

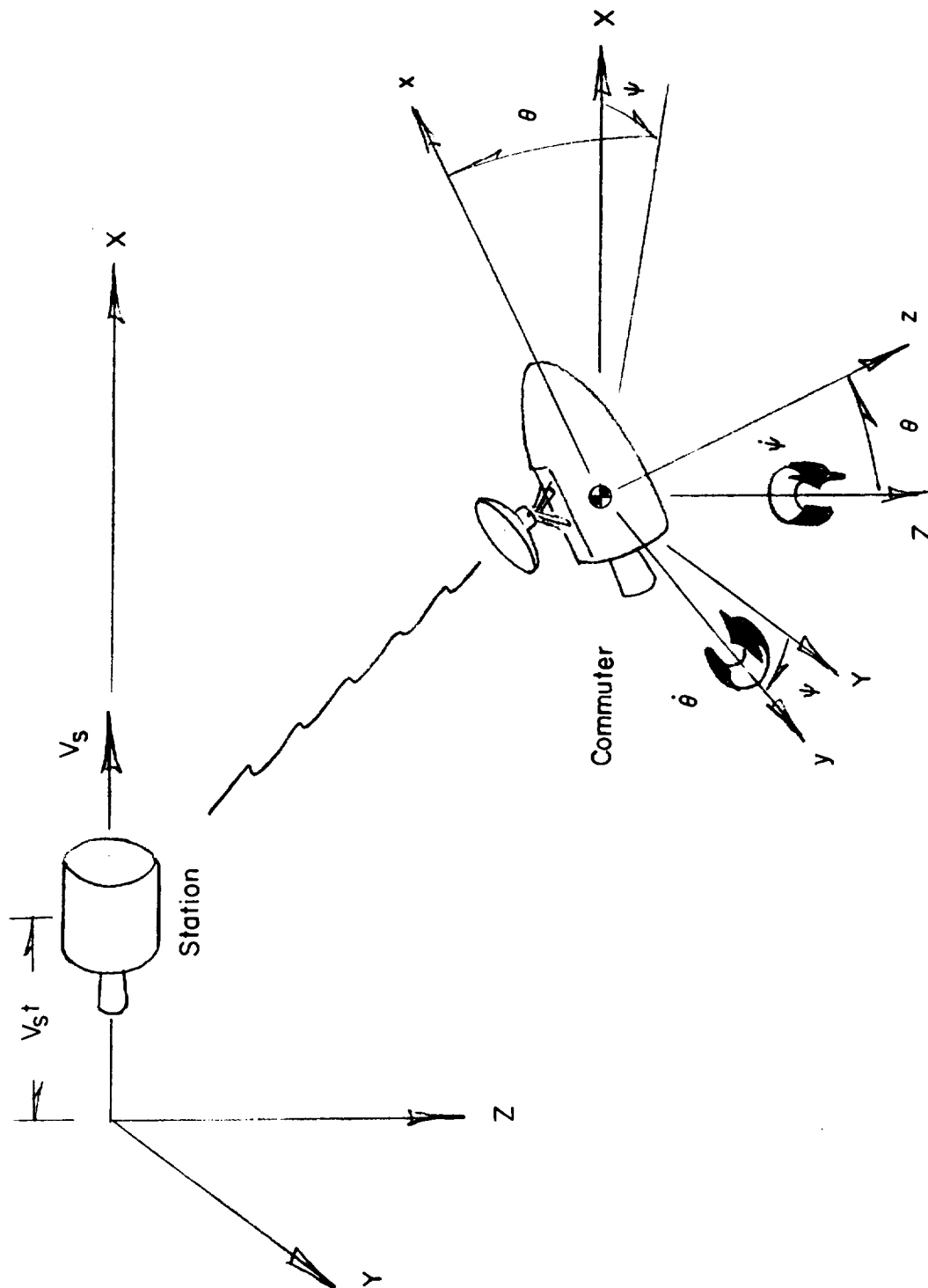


Figure 1.- Axes used in investigation.  $X, Y, Z$  axes have origin at the space station at  $t = 0$ . Euler angle order of rotation is  $\psi, \theta$ .

L-1522

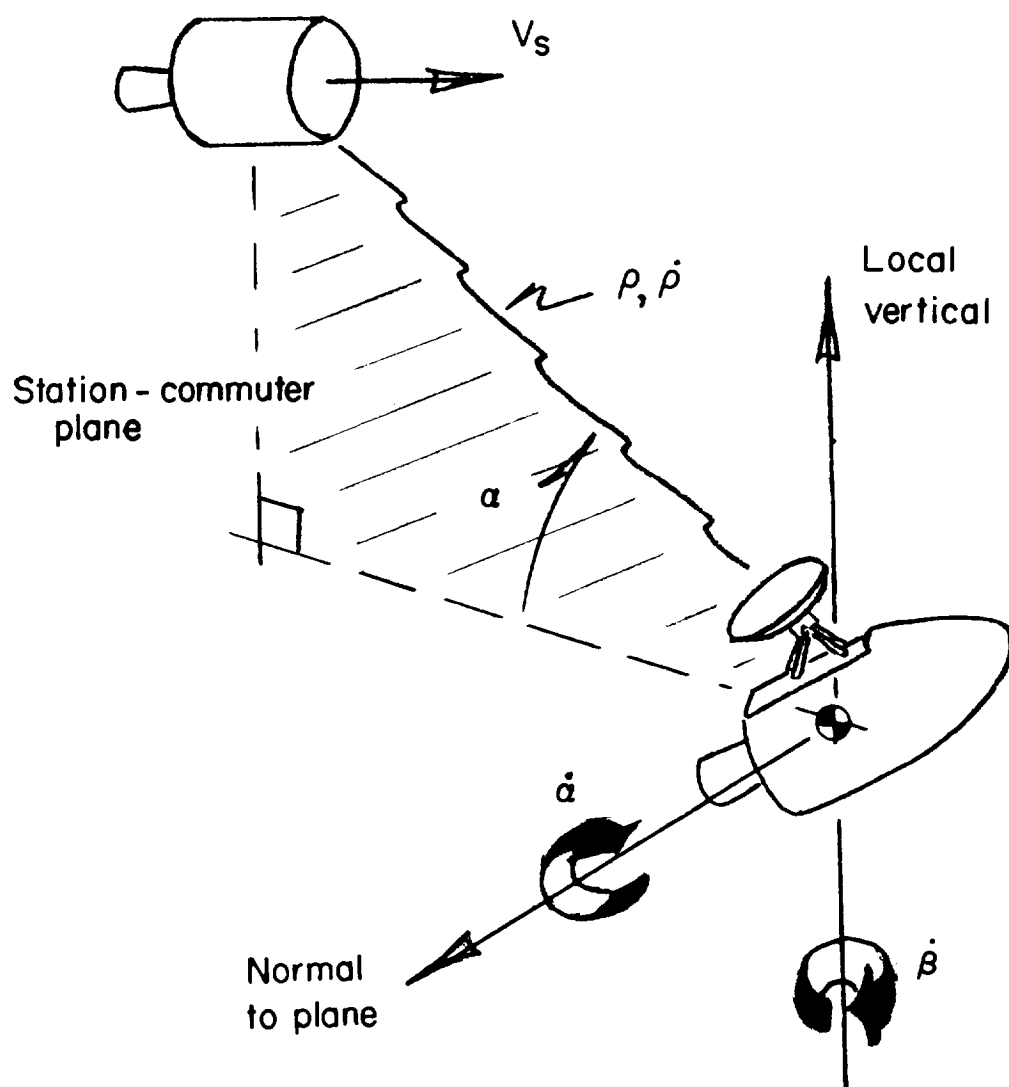


Figure 2.- Information inputs required for guidance scheme.

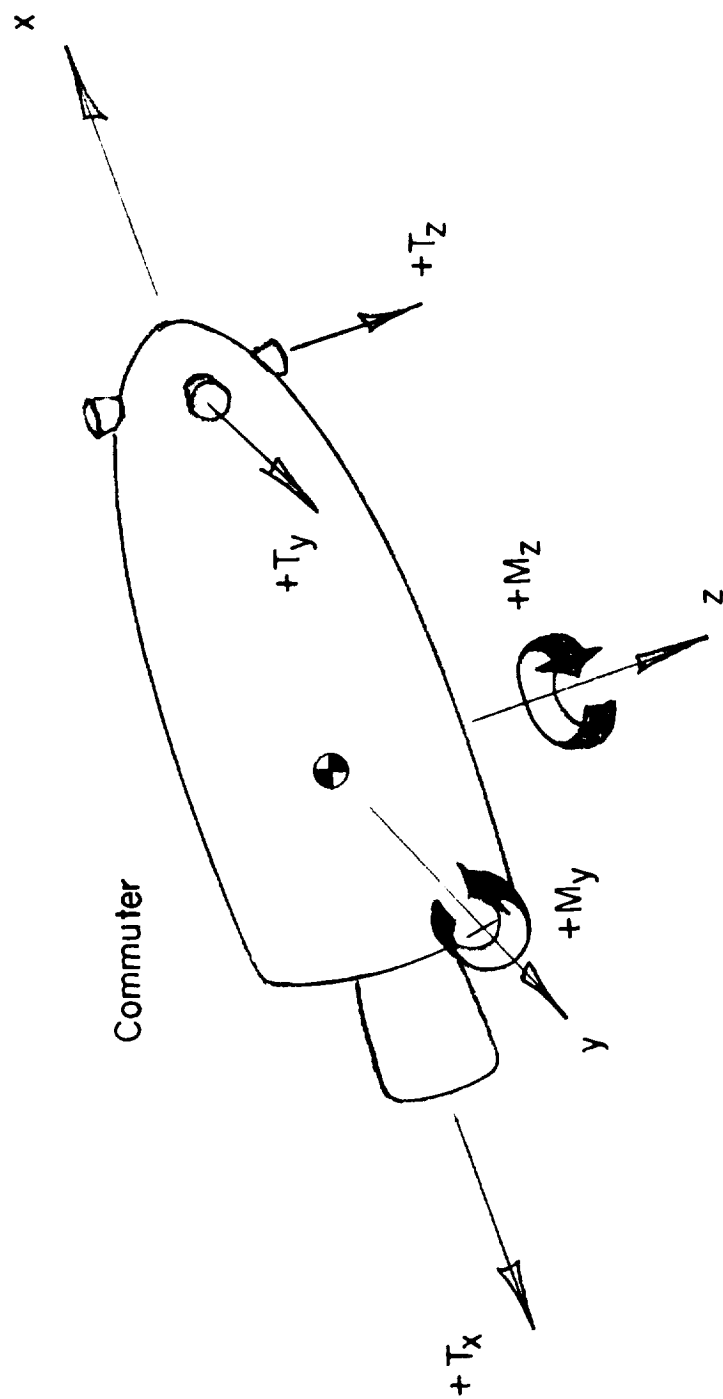
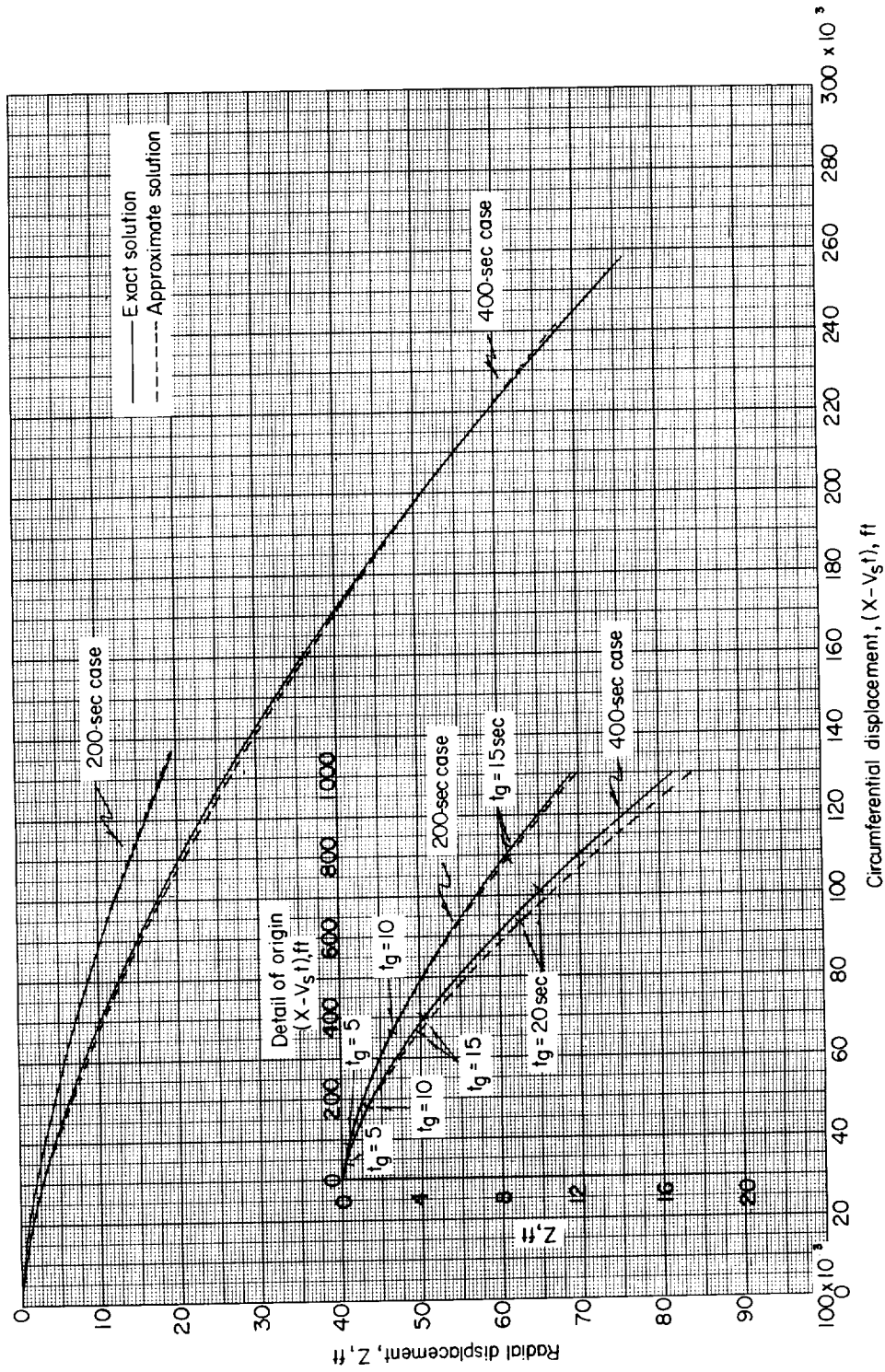
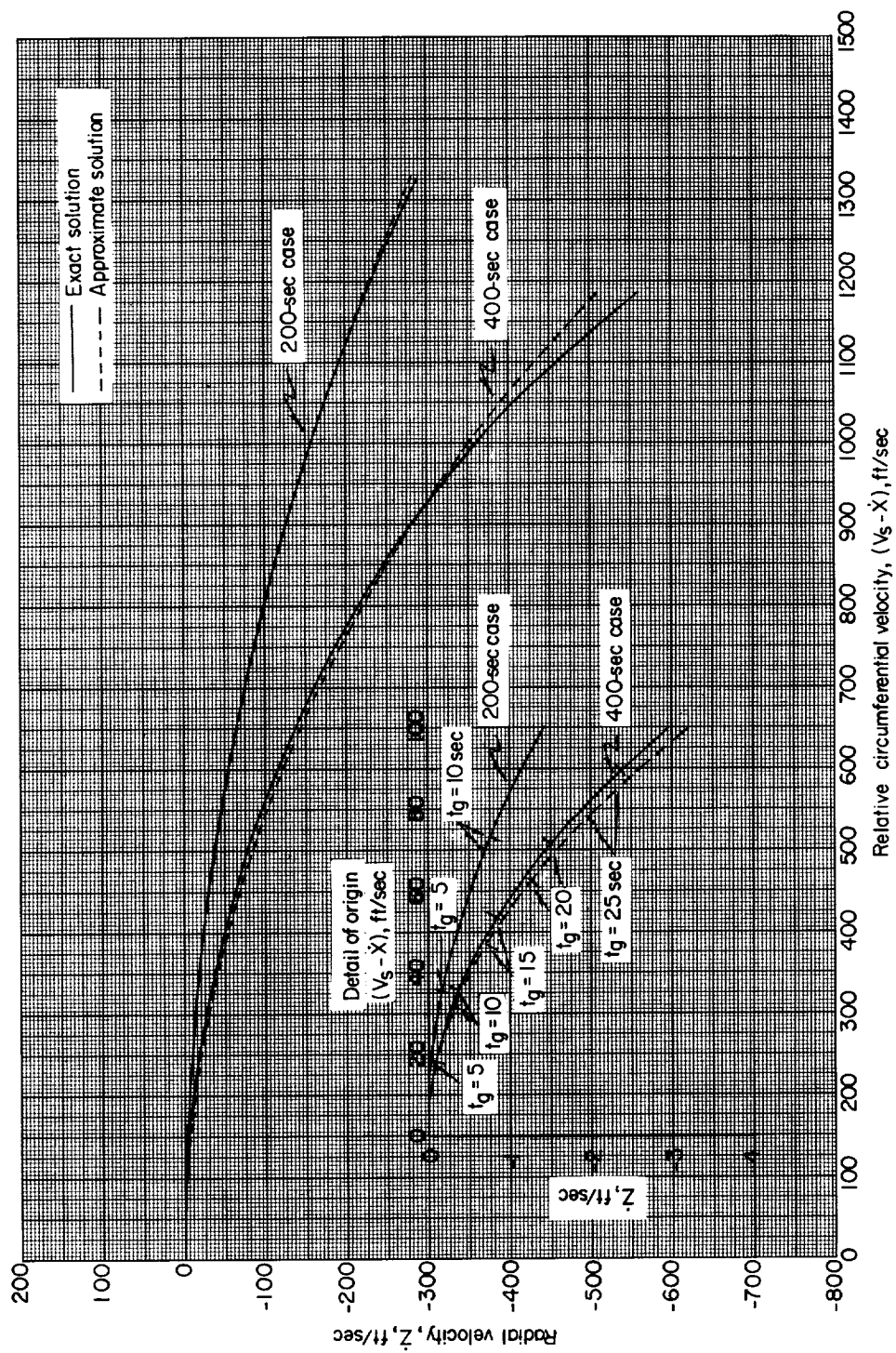


Figure 3.- Force and moment definitions for thrust and attitude control configuration. Arrows indicate positive direction.



(a) Displacement profile.

Figure 4.- Comparison of rendezvous displacement and relative velocity profiles from exact calculations and assumed rectangular representation for matched initial circumferential velocities with 200- and 400-second terminal-stage burning times.



(b) Velocity profile.

Figure 4.- Concluded.



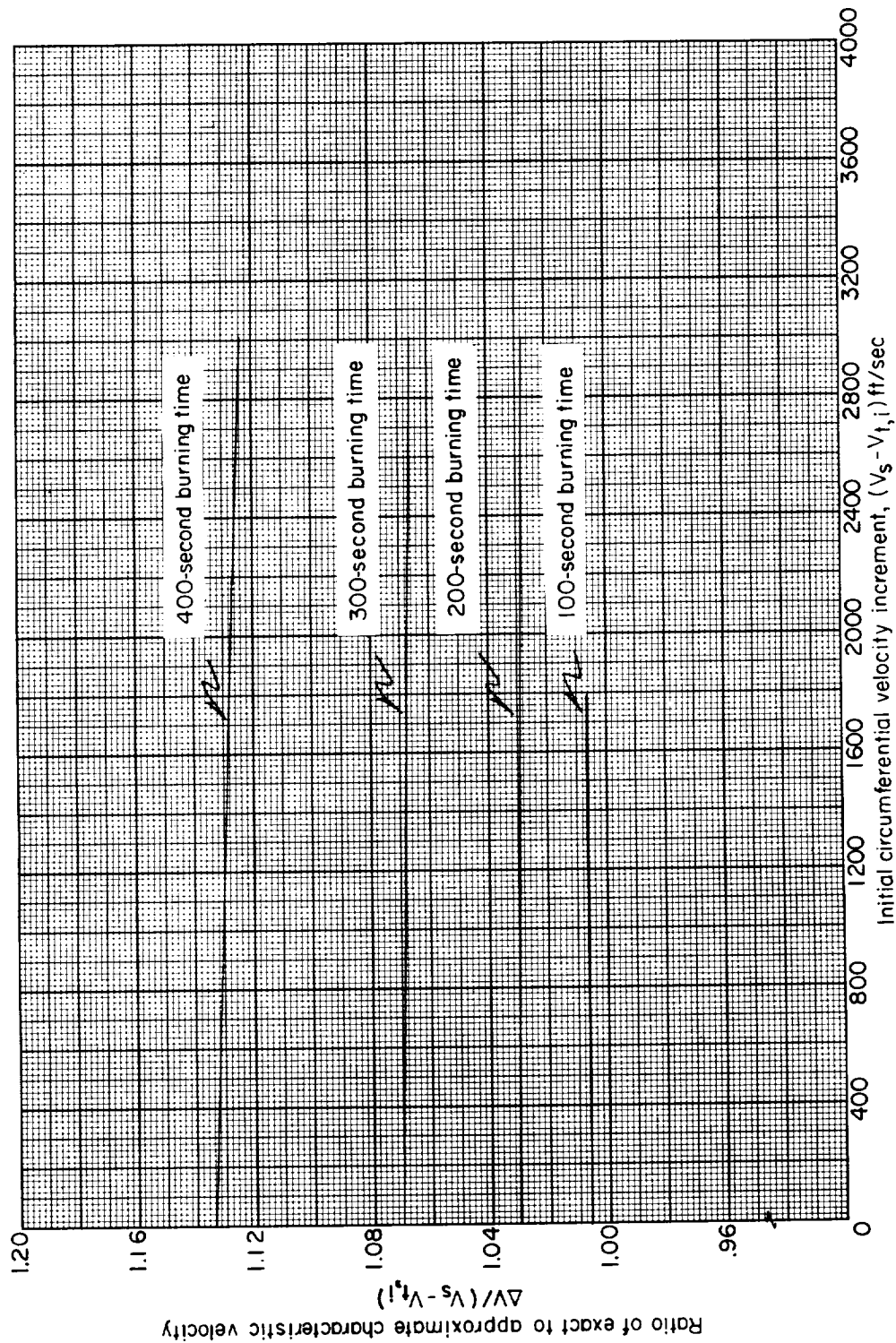
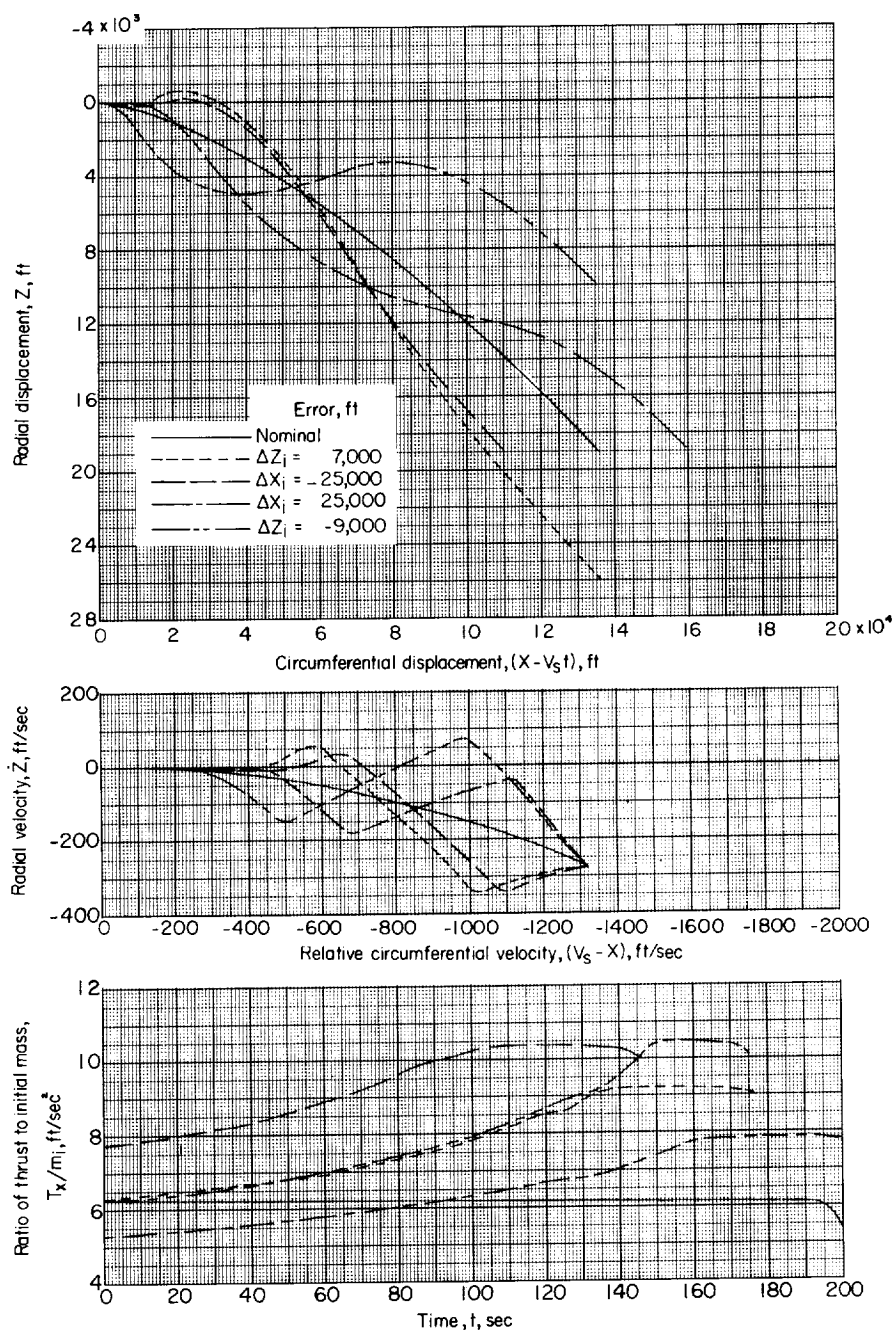


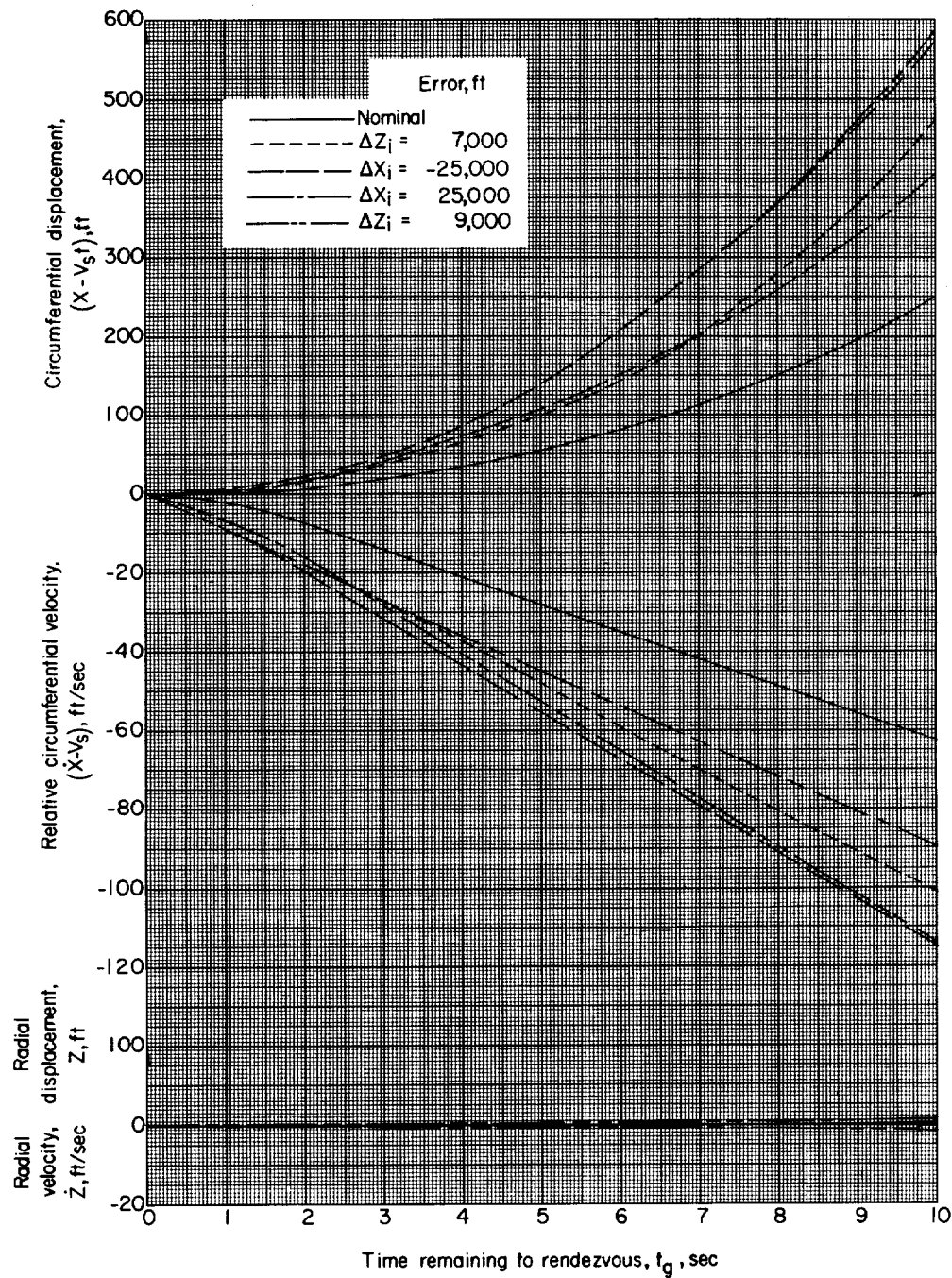
Figure 5.- Variation of ratio of exact to approximate characteristic velocity with initial circumferential velocity from exact calculations for coplanar rendezvous with station in 400-nautical-mile circular orbit.  $c = 10,000$  ft/sec.



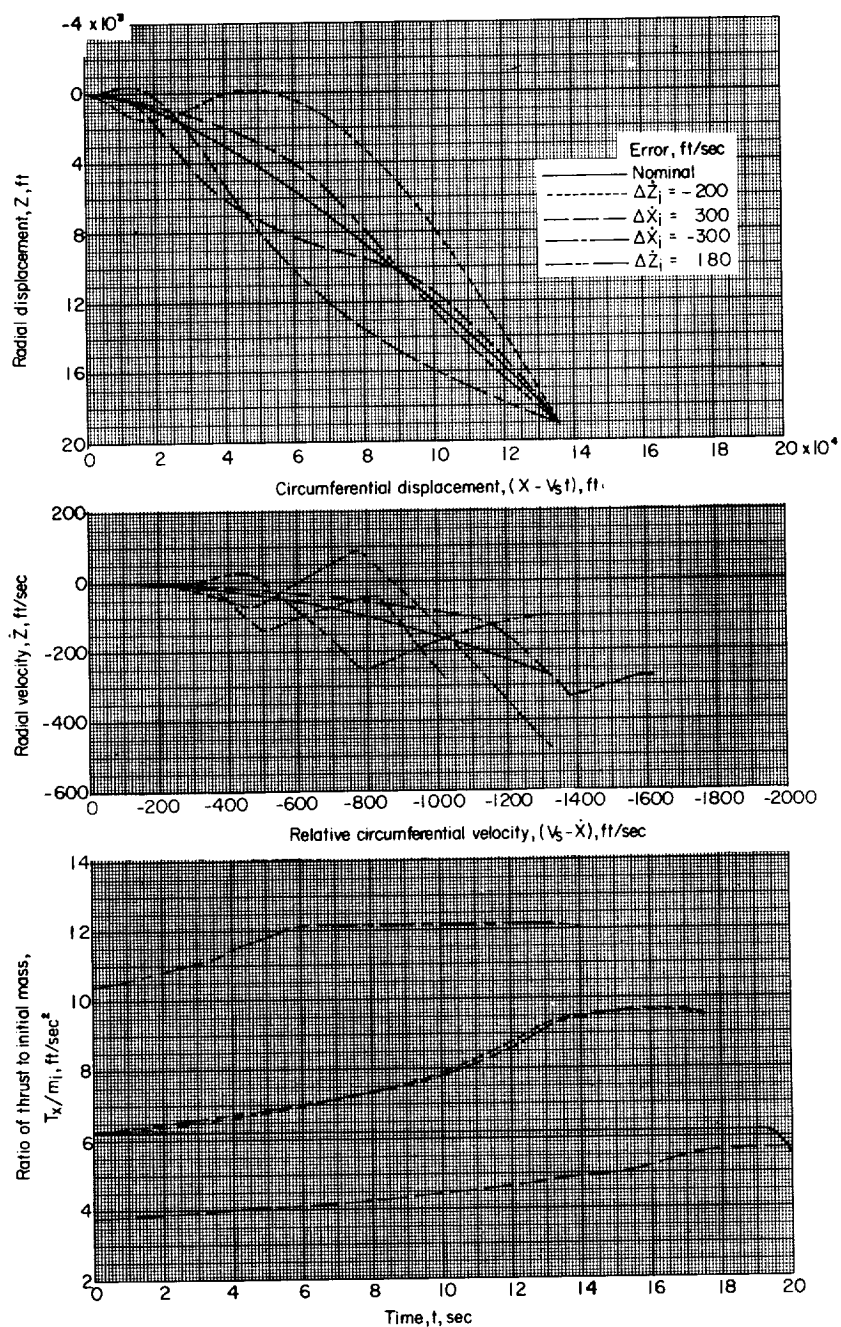


(a) Relative geometry and thrust variation.

Figure 7.- Coplanar rendezvous for nominal and extreme initial errors in displacement. Nominal terminal-stage burning time of 200 seconds for rendezvous with station in 400-nautical-mile circular orbit.

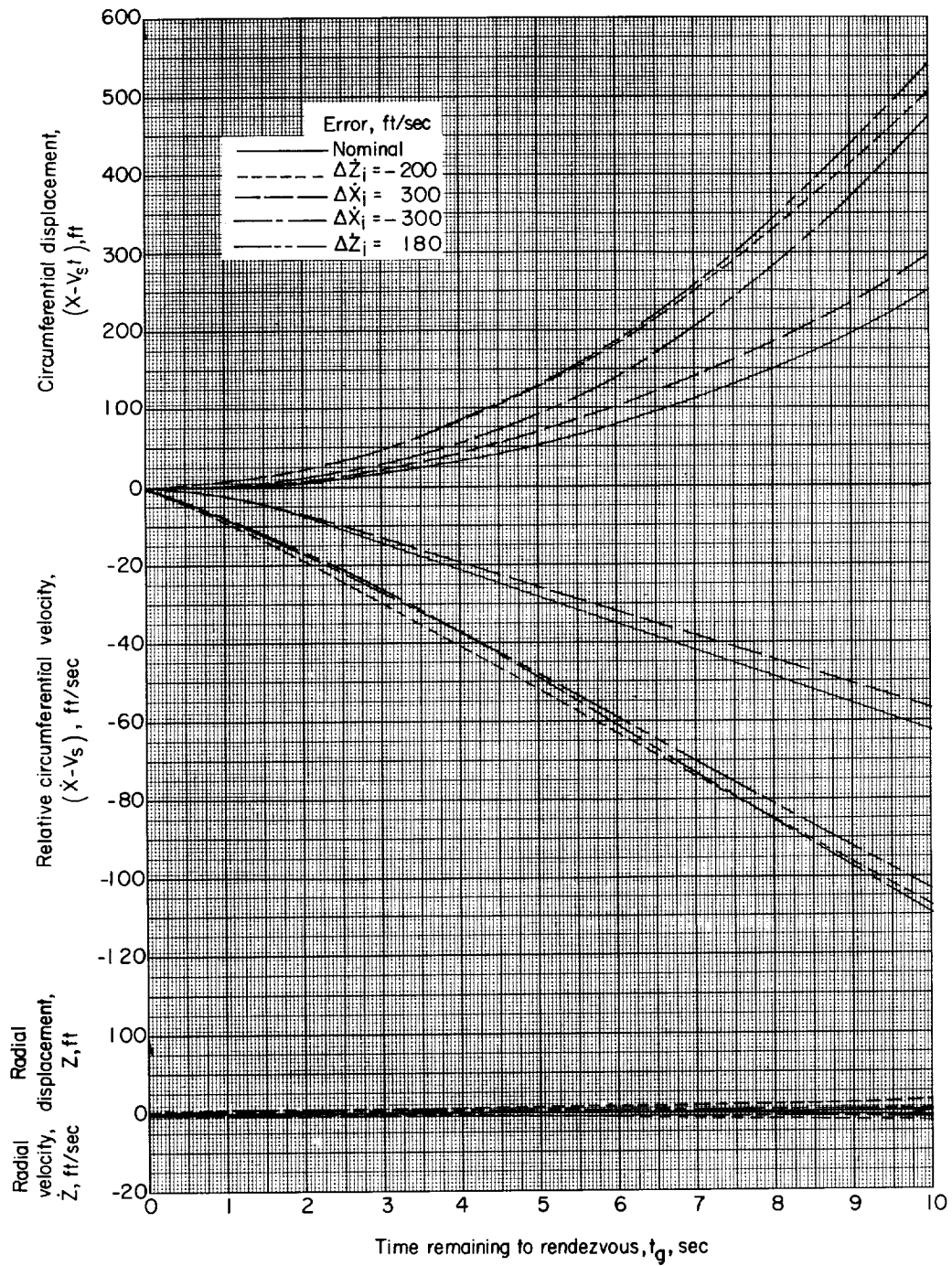


(b) Time history of final 10 seconds before rendezvous.



(a) Relative geometry and thrust variation.

Figure 8.- Coplanar rendezvous for nominal and extreme initial errors in velocity. Nominal terminal-stage burning time of 200 seconds for rendezvous with station in 400-nautical-mile circular orbit.



(b) Time history of final 10 seconds before rendezvous.

Figure 8.- Concluded.



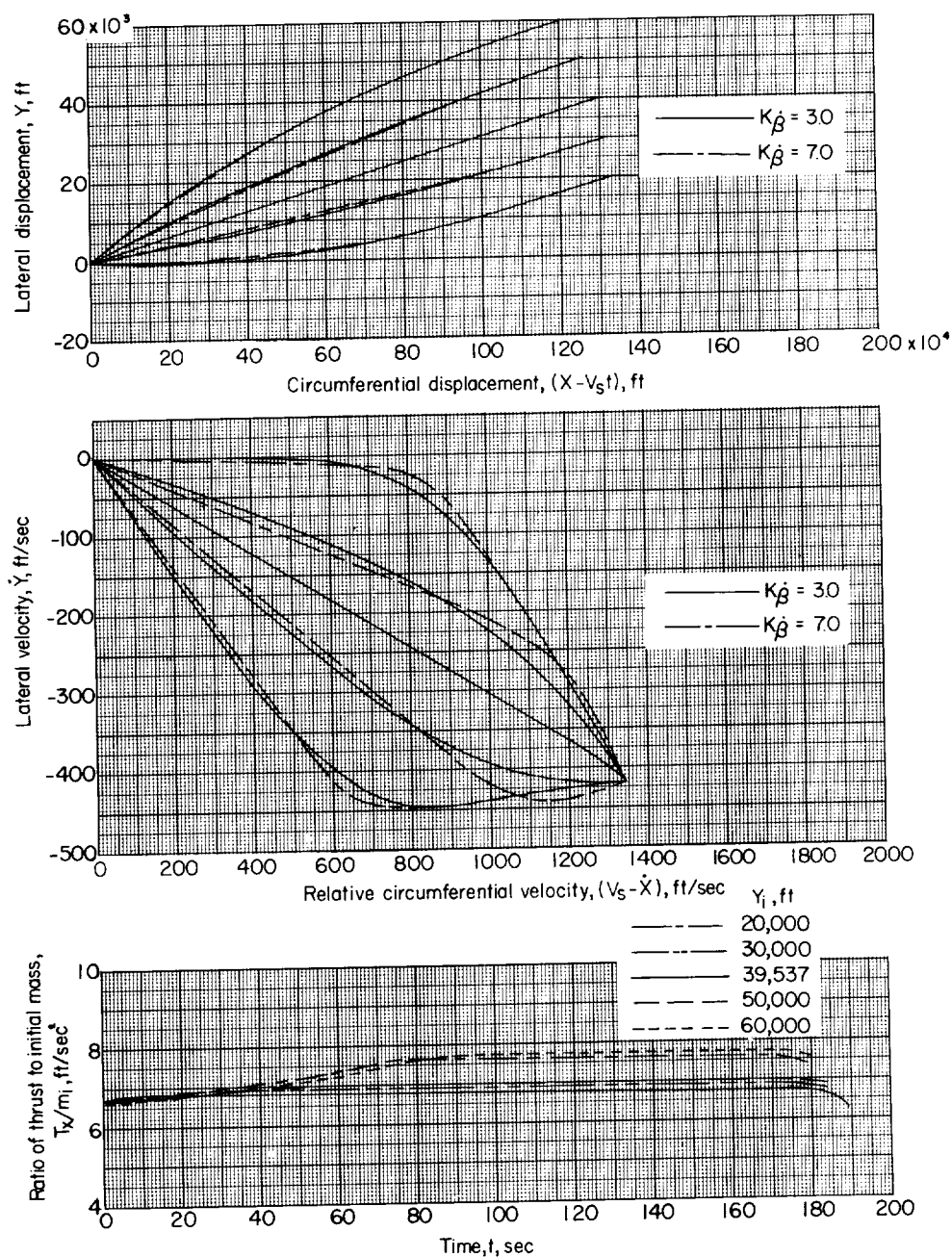


Figure 9.- Relative geometry and thrust variation in cross-plane rendezvous for lateral velocity offset of  $1^\circ$ , various initial lateral displacements, and  $K_{\dot{\beta}} = 3.0$  and  $7.0$ . Nominal terminal-stage burning time of 200 seconds for rendezvous with station in 400-nautical-mile circular orbit.

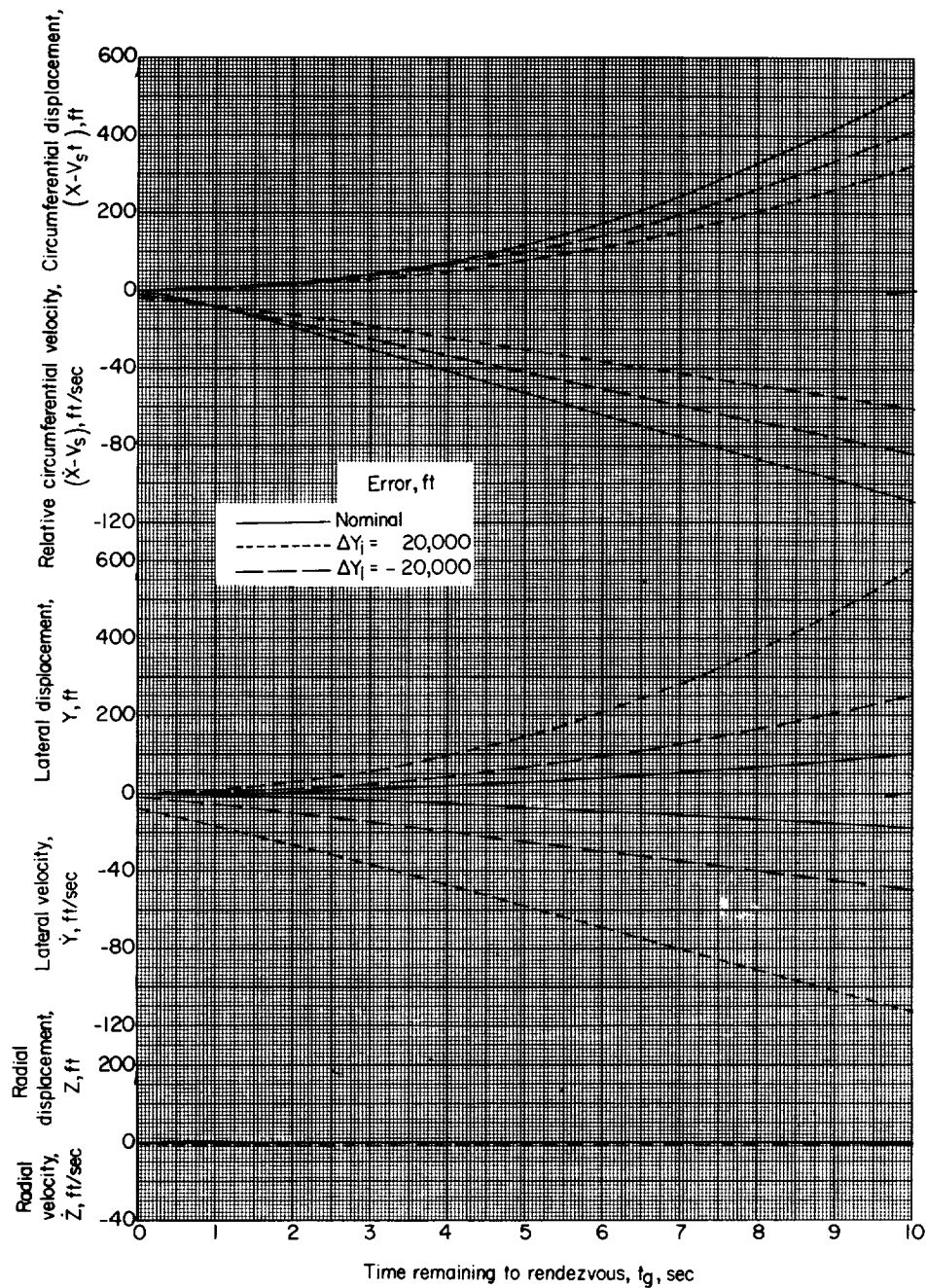
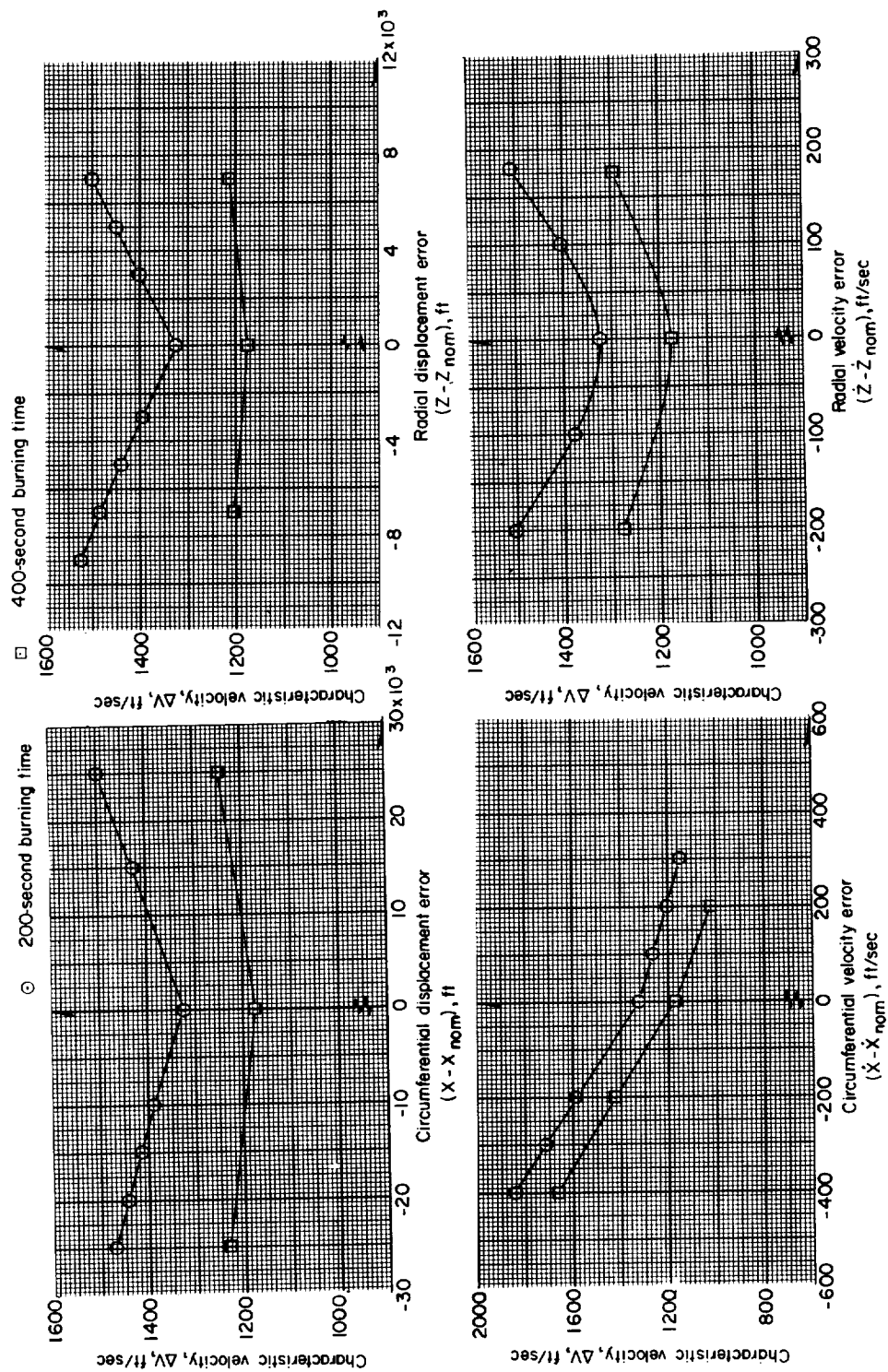


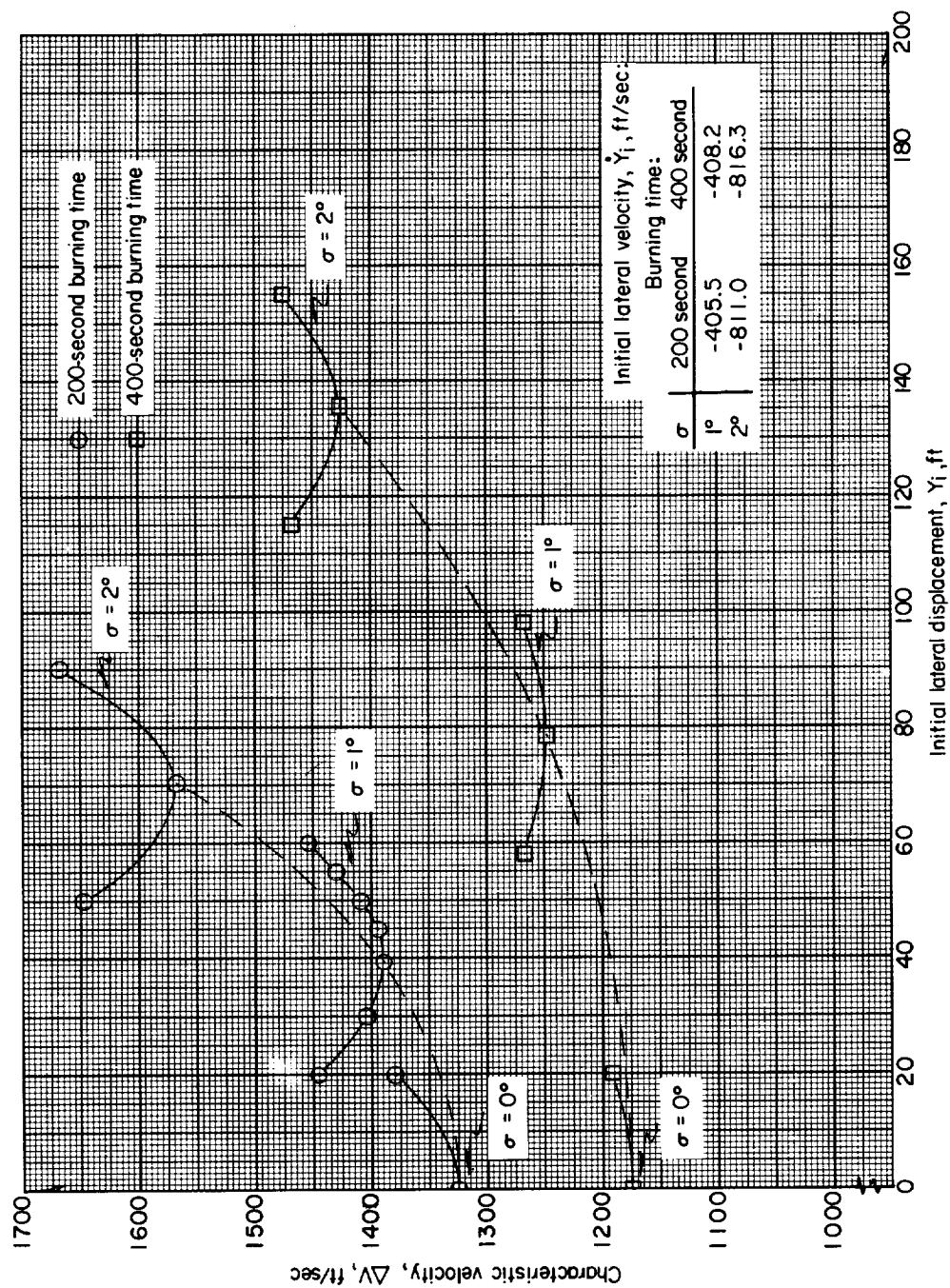
Figure 10.- Time history of final 10 seconds before rendezvous for initial lateral velocity offset of  $2^\circ$  at nominal initial lateral offset, extreme initial displacement errors, and  $K_p = 3.0$ . Nominal terminal-stage burning time of 200 seconds for rendezvous with station in 400-nautical-mile circular orbit.





(a) Initial in-plane errors.

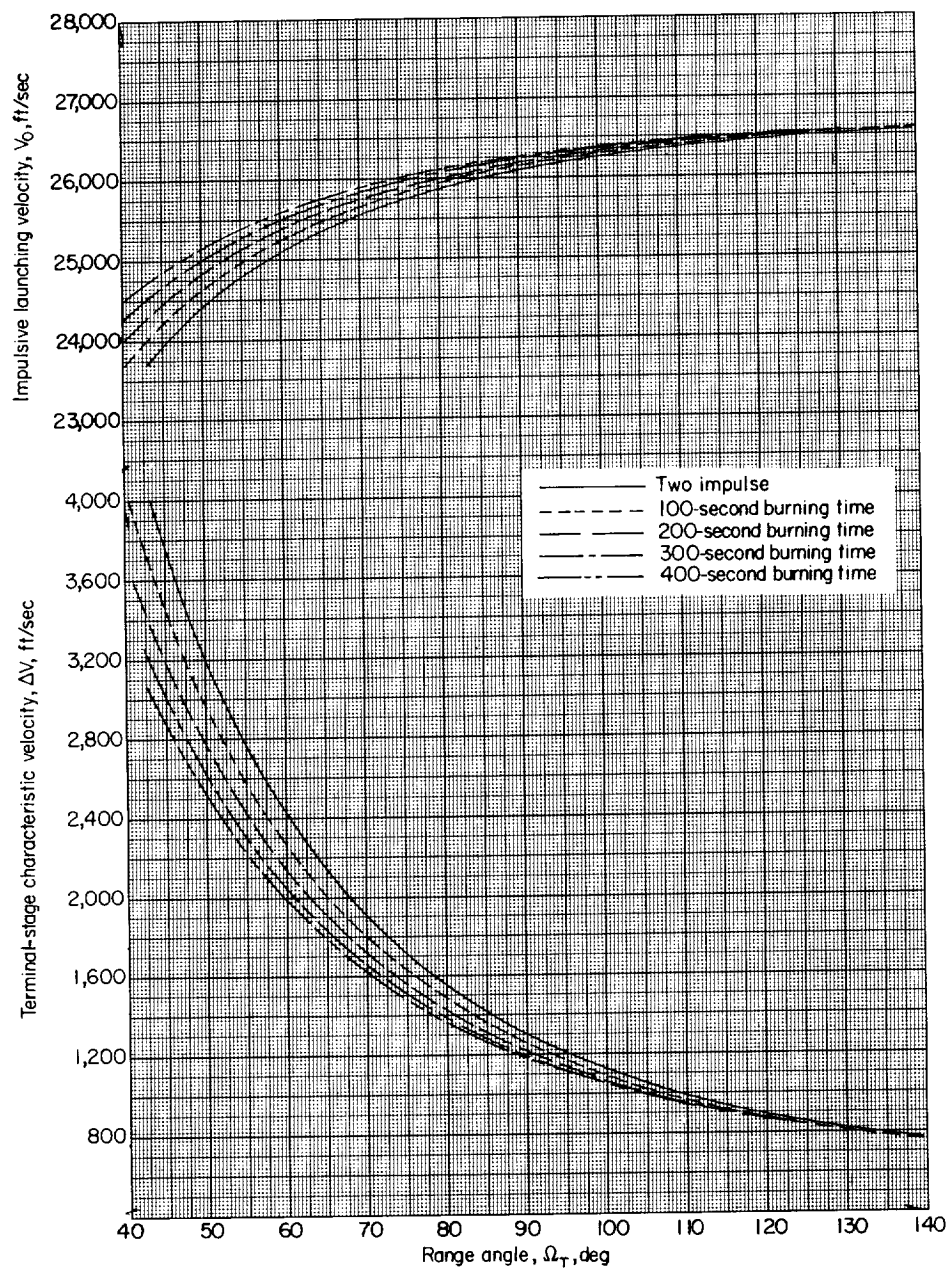
Figure 11.- Variation of required characteristic velocity with initial in-plane errors and cross-plane displacements for burning times of 200 and 400 seconds.



(b) Initial cross-plane displacements for lateral velocity offsets of  $0^\circ$ ,  $1^\circ$ , and  $2^\circ$ .

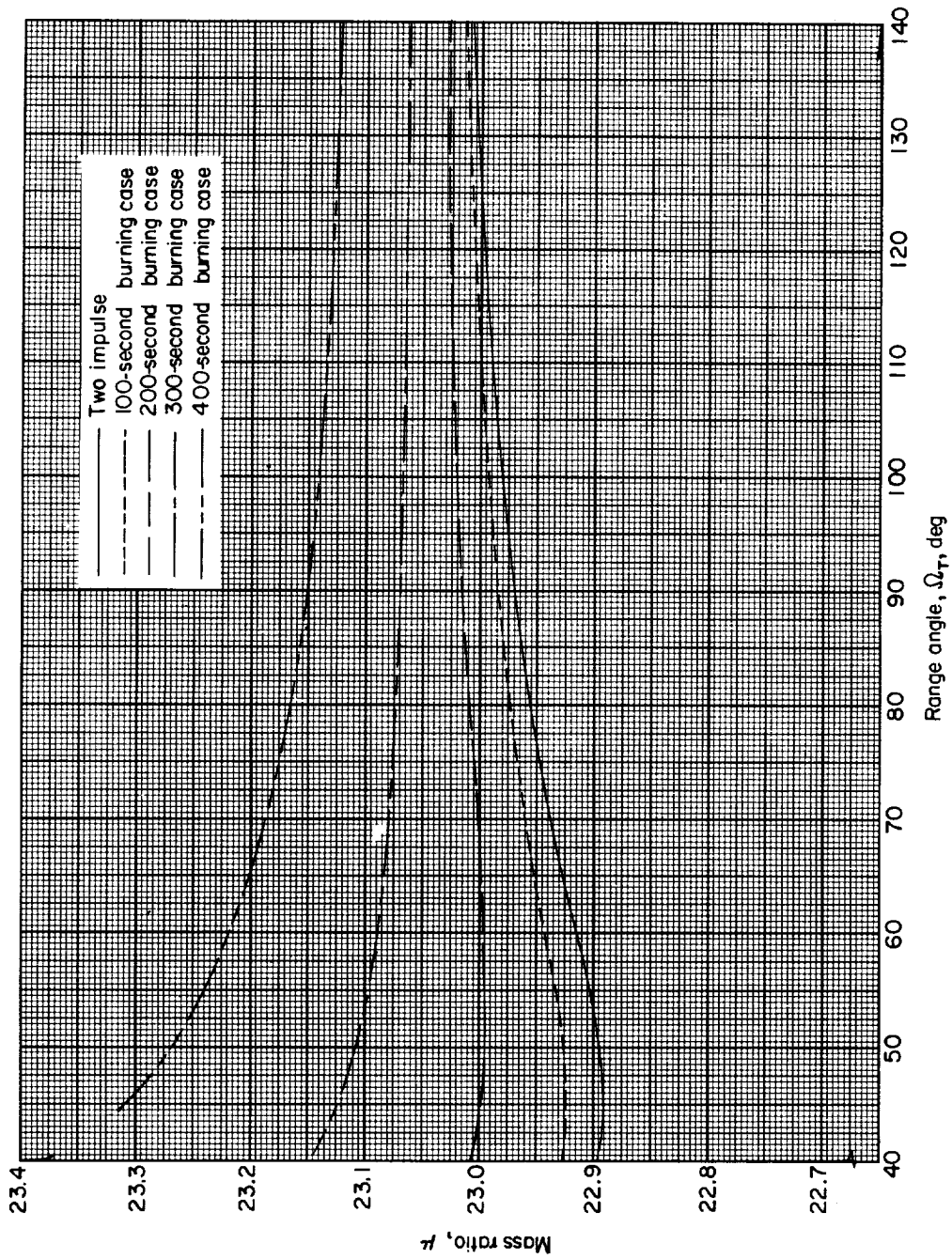
Figure 11.- Concluded.

L-1522



(a) Required characteristic velocities.

Figure 12.- Characteristic velocity and variation of mass ratio for two-impulse coplanar transfer and finite terminal-stage burning times of 100, 200, 300, and 400 seconds.



(b) Mass ratio variation.

Figure 12.- Concluded.

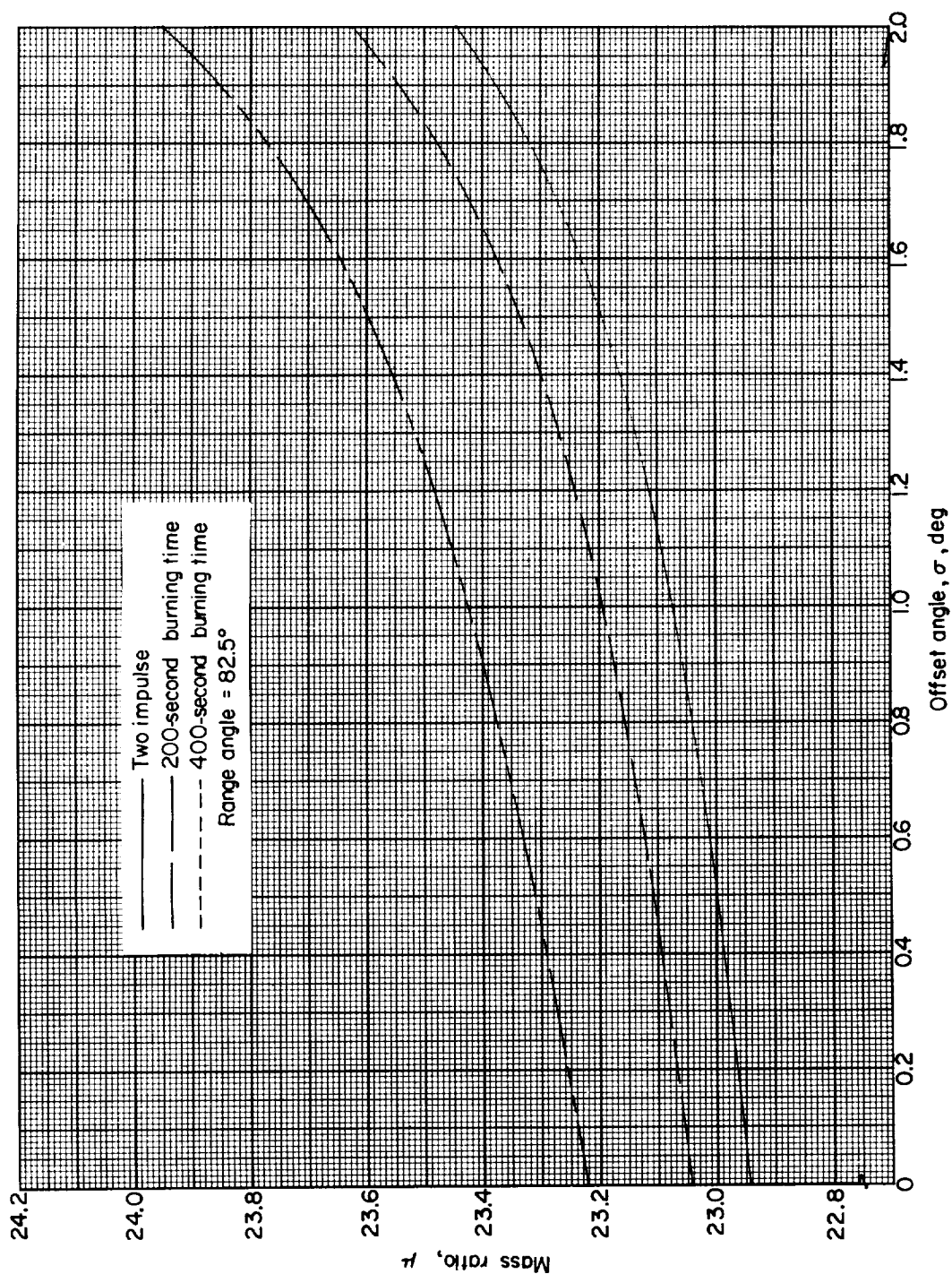


Figure 13.- Mass ratio variation with lateral velocity offset angle for two-impulse case and terminal-stage burning times of 200 and 400 seconds.



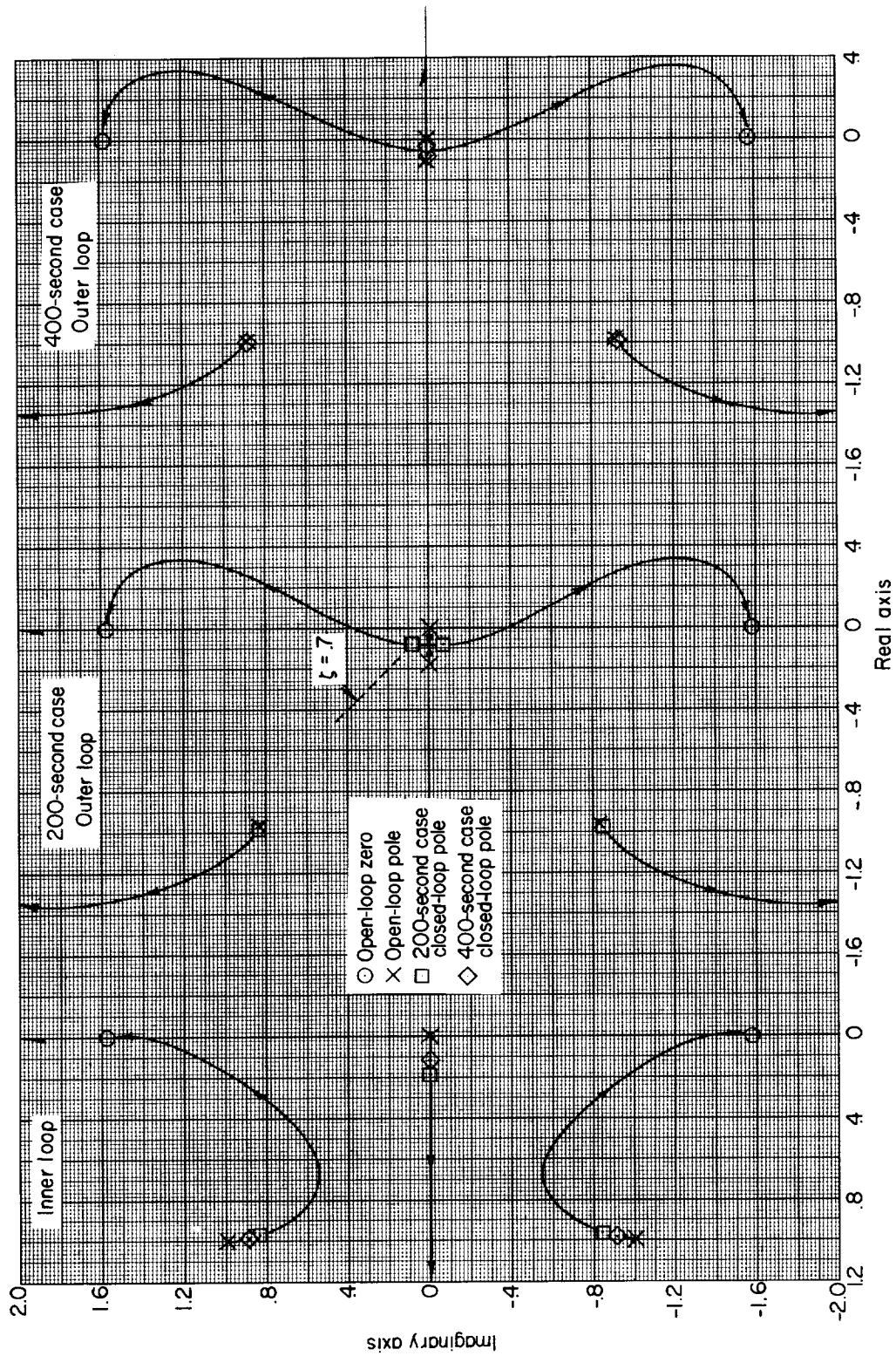


Figure 14.- Root locus for linearized longitudinal controller.

<p>NASA TN D-923 National Aeronautics and Space Administration. AN AUTOMATIC TERMINAL GUIDANCE SYSTEM FOR RENDEZVOUS WITH A SATELLITE. Terrance M. Carney. August 1961. 68p. OTS price, \$1.75. (NASA TECHNICAL NOTE D-923)</p> <p>A steering and control system for automatic terminal guidance in direct-ascent satellite rendezvous, using control of thrust magnitude and direction, is presented and analyzed in this paper. For a representative case, rendezvous with a station in a 400-nautical-mile circular orbit, the range of initial velocity and displacement errors which the system is able to correct is determined. Generalized considerations for efficient use of such a system are examined.</p>	<p>I. Carney, Terrance M. II. NASA TN D-923</p> <p>(Initial NASA distribution: 22, Guidance and homing systems; 46, Space mechanics; 47, Satellites.)</p>	<p>NASA</p>
<p>NASA TN D-923 National Aeronautics and Space Administration. AN AUTOMATIC TERMINAL GUIDANCE SYSTEM FOR RENDEZVOUS WITH A SATELLITE. Terrance M. Carney. August 1961. 68p. OTS price, \$1.75. (NASA TECHNICAL NOTE D-923)</p> <p>A steering and control system for automatic terminal guidance in direct-ascent satellite rendezvous, using control of thrust magnitude and direction, is presented and analyzed in this paper. For a representative case, rendezvous with a station in a 400-nautical-mile circular orbit, the range of initial velocity and displacement errors which the system is able to correct is determined. Generalized considerations for efficient use of such a system are examined.</p>	<p>I. Carney, Terrance M. II. NASA TN D-923</p> <p>(Initial NASA distribution: 22, Guidance and homing systems; 46, Space mechanics; 47, Satellites.)</p>	<p>NASA</p>
<p>NASA TN D-923 National Aeronautics and Space Administration. AN AUTOMATIC TERMINAL GUIDANCE SYSTEM FOR RENDEZVOUS WITH A SATELLITE. Terrance M. Carney. August 1961. 68p. OTS price, \$1.75. (NASA TECHNICAL NOTE D-923)</p> <p>A steering and control system for automatic terminal guidance in direct-ascent satellite rendezvous, using control of thrust magnitude and direction, is presented and analyzed in this paper. For a representative case, rendezvous with a station in a 400-nautical-mile circular orbit, the range of initial velocity and displacement errors which the system is able to correct is determined. Generalized considerations for efficient use of such a system are examined.</p>	<p>I. Carney, Terrance M. II. NASA TN D-923</p> <p>(Initial NASA distribution: 22, Guidance and homing systems; 46, Space mechanics; 47, Satellites.)</p>	<p>NASA</p>
<p>NASA TN D-923 National Aeronautics and Space Administration. AN AUTOMATIC TERMINAL GUIDANCE SYSTEM FOR RENDEZVOUS WITH A SATELLITE. Terrance M. Carney. August 1961. 68p. OTS price, \$1.75. (NASA TECHNICAL NOTE D-923)</p> <p>A steering and control system for automatic terminal guidance in direct-ascent satellite rendezvous, using control of thrust magnitude and direction, is presented and analyzed in this paper. For a representative case, rendezvous with a station in a 400-nautical-mile circular orbit, the range of initial velocity and displacement errors which the system is able to correct is determined. Generalized considerations for efficient use of such a system are examined.</p>	<p>I. Carney, Terrance M. II. NASA TN D-923</p> <p>(Initial NASA distribution: 22, Guidance and homing systems; 46, Space mechanics; 47, Satellites.)</p>	<p>NASA</p>

